THE ASTROPHYSICAL JOURNAL, 292:29–48, 1985 May 1

OPTICAL EMISSION-LINE PROPERTIES OF EVOLVED GALACTIC SUPERNOVA REMNANTS

ROBERT A. FESEN[1]
Laboratory for Astronomy and Solar Physics, NASA/Goddard Space Flight Center
WILLIAM P. BLAIR
Harvard-Smithsonian Center for Astrophysics
AND
ROBERT P. KIRSHNER
Department of Astronomy, University of Michigan
Received 1984 August 21; accepted 1984 November 16

ABSTRACT

New optical spectrophotometric data are presented for the supernova remnants CTB 1, OA 184, VRO 42.05.01, S147, the Monoceros Loop, G206.9+2.3, and G65.3+5.7. These data are combined with published spectral data to study some of the general properties of evolved galactic supernova remnants. We find that (1) [O I] and [O II] line strengths, when used in conjunction with the usual Hα/[S II] ratio test, provide an excellent additional diagnostic for discriminating remnants from H II regions; (2) the line ratios Hα/[N II], Hα/[S II], and [S II] λ6717/λ6731 generally do not vary substantially among the filaments of an individual remnant; and (3) the observed correlation of [N II]/Hα with [S II] λ6717/λ6731 in remnants is the result of observational selection rather than of evolutionary effects. We derive a galactic nitrogen abundance gradient of $d \log (N/H)/dR = -0.088$ dex kpc^{-1}, which is in agreement with that derived from H II regions. However, no abundance gradients for oxygen or sulfur are indicated from the remnant data.

Subject headings: nebulae: abundances — nebulae: H II regions — nebulae: supernova remnants — spectrophotometry

I. INTRODUCTION

At present there are approximately 150 known galactic supernova remnants (SNRs). The great majority of these are believed to be relatively old and evolved objects in either the adiabatic or the early radiative stages of their evolutionary development (Woltjer 1972). Such old remnants have ages greater than 10^3 years and radii larger than ~5 pc, and generally show a characteristic shell structure of nonthermal radio emission.

About three dozen galactic SNRs have known optical emission associated with their nonthermal radio emission (van den Bergh 1983). For old remnants this optical emission arises from the cooling of shocked interstellar cloud material following passage of the remnant's blast wave as it expands outward into the ambient medium. Spectra of filaments of evolved SNRs over the wavelength range 3500–7500 Å show strong lines of H, [O II], [O III], [S II], and [N II] with generally fainter lines of He I, He II, [O I], [N I], [Ne III], [Fe II], [Fe III], [Ca II], and [Ar III]. In contrast to the situation for young remnants such as Cas A and the Crab Nebula, where there is elemental enrichment from the supernova ejecta, older SNR abundances seem to reflect that of the ambient interstellar medium, although with varying degrees of grain destruction (Raymond 1983; Seab and Shull 1983).

Although a few evolved remnants have been well studied optically (e.g., the Cygnus Loop [Miller 1974; Fesen, Blair, and Kirshner 1982; Hester, Parker, and Dufour 1983]), relatively few spectral data are available on many of the fainter optical remnants. This is due in part to the difficulty of obtaining good-quality spectra on the fainter nebulae, as well as to the concentration by investigators on the bright prototype objects which have been well studied at other frequencies. A more complete sampling of the optical line emissions in galactic SNRs would allow the study of (1) additional criteria besides the Hα/[S II] ratio for distinguishing shocked nebulae from photoionized nebulae, (2) the range of line-emission strengths found within an individual remnant, (3) whether there are significant evolutionary variations in a remnant's optical emission properties as a function of remnant diameter, and (4) the galactic elemental abundance gradients using SNRs.

Toward these objectives, we obtained new optical spectrophotometry of seven relatively faint optical galactic SNRs. The remnants are CTB 1, OA 184, VRO 42.05.01, S147, the Monoceros Loop, G206.9+2.3, and G65.3+5.7. For many of these remnants, these new data represent a considerable improvement in quality and spectral coverage over those previously available. Combining these data with those already published, we present an overview of some general optical emission-line properties for evolved galactic SNRs.

II. OBSERVATIONS

Spectrophotometric observations of the seven SNRs were obtained with the 2000 channel digital spectrometer attached to the 1.3 m telescope at McGraw-Hill Observatory on Kitt Peak. This instrument uses a Reticon detector, six stages of image intensification, and pulse-centroiding electronics. Table 1 lists the coordinates, slit sizes, spectral coverage, and integration time for each of the various observations. Precise slit locations are shown in Figure 1. Accurate slit positioning and guiding were accomplished with the aid of a three-stage intensified television guider. Sky measurements with integration times equal to those for the filaments were taken at neighboring blank field locations.

[1] Also Laboratory for Atmospheric and Space Physics, University of Colorado.

TABLE 1

LOG OF OBSERVATIONS

SNR AND POSITION	COORDINATES (1950) R.A.	Decl.	APERTURE (arcsec)	INTEGRATION TIME (s)	SPECTRAL COVERAGE (Å)
CTB 1	23^h54^m6	+61°59′	3 × 40	2000	3700–7400
OA 184	05 13.9	+42 08	4 × 40	8100	4000–7500
VRO 42.05.01	05 22.3	+43 04	4 × 40	1800	4000–7500
S147:					
Position 1	05 39.7	+28 20	3 × 40	3000	3700–7400
Position 2	05 35.3	+27 37	3 × 40	3600	3700–7400
Position 3	05 41.8	+28 22	3 × 40	3000	3700–7400
Position 4	05 35.7	+26 24	3 × 40	4800	3700–7400
Position 5	05 31.3	+27 57	3 × 40	4800	3700–7400
Monoceros Loop:					
Position 1	06 30.1	+06 36	3 × 40	3300	3700–7400
Position 2	06 40.5	+06 18	4 × 40	5400	3700–7400
G206.9+2.3:					
Position 1	06 46.8	+06 44	3 × 40	2100	4000–7000
Position 2	06 46.6	+06 01	4 × 40	3000	4000–7000
G65.3+5.7:					
Position 1	19 37.0	+29 51	3 × 40	5700	3700–7400
Position 2	19 41.1	+31 36	3 × 40	6000	3700–7400

Data reduction was accomplished using observations of Oke's (1974) white dwarfs for measuring the instrumental spectral response and He, Ne, Ar, and Kr comparison lamps for wavelength calibration. The reduced spectra are shown in Figure 2. Observed line fluxes relative to Hβ are listed in Table 2, along with reddening-corrected line strengths assuming an intrinsic Hα/Hβ ratio of 3.0 and using the Whitford reddening curve as given by Miller and Mathews (1972). Because these data were taken over several years under various observing conditions and on filaments of widely differing brightness, the accuracy of the measured line strengths is not uniform (e.g., note the varying signal-to-noise ratios for the spectra; see Fig. 2). However, the relative line intensities for the stronger lines should be accurate to $\pm 25\%$ or better, with the exception of G206.9+2.3, where the errors may be as large as $\pm 50\%$.

III. RESULTS ON INDIVIDUAL OBJECTS

Below is a brief discussion of our spectral data for each remnant. Electron density estimates via the [S II] λ6717/λ6731 line ratio have been derived using Pradhan's (1978) cross sections and Mendoza and Zeippen's (1982) A-values (see Fig. 6 of Blair and Kirshner 1985). Although many of these remnants have been previously observed (e.g., D'Odorico and Sabbadin 1977), none had optical extinction estimates, because of a lack of blue spectral coverage. We list in Table 3 our estimated visual reddening values, A_V (where $A_V = 3.0 \times E_{B-V}$), along with implied distances using the general galactic absorption versus distance studies of FitzGerald (1968), Lucke (1978), and Neckel and Klare (1980). The resulting distance estimates are consistent with those derived by Clark and Caswell (1976) using the empirical Σ-D relation, except in the case of G206.9+2.3 (see § III*f* below).

a) CTB 1 (G117.3+0.1)

Previously published spectra of this remnant were obtained by D'Odorico and Sabbadin (1977) and Bohigas *et al.* (1983). The D'Odorico and Sabbadin spectra were taken at eight locations along the remnant's southern rim in the wavelength region 6000–6800 Å, from which they reported only minor variations in the Hα/[N II] and Hα/[S II] line ratios. Our data were also taken along the southwestern rim near their positions 7 and 8, and our Hα/[N II] and Hα/[S II] ratios of 1.31 and 0.82 are in fair agreement with their reported average values of 1.62 and 1.0. Our measured [S II] λ6717/λ6731 ratio of 1.33 suggests a electron density value near 100 cm^{-3}. However, larger ratio values are reported by Bohigas *et al.* (1983), who find Hα/[N II] = 1.87–2.70, with Hα/[S II] = 1.46–2.73 for six filaments in the same region.

From the photographs of Parker, Gull, and Kirshner (1979), the [O III]/Hβ ratio of CTB 1 is likely to be greater along its western rim than the value of $\sim$1.0 that we observed at our southwest position. A low signal-to-noise spectrum of a western filament (not shown) indeed indicates [O III]/H$\beta \geq 15$.

b) OA 184 (G166.2+2.5)

This remnant, which appears optically as a broken shell of diffuse emission about 70′ × 90′ in size, is notable for exhibiting line-emission strengths unlike those seen in other remnants. D'Odorico and Sabbadin's (1977) spectra of seven of the brightest regions along the diffuse optical shell indicated abnormally weak [S II] emission (Hα/[S II] near 3.0) and λ6717/λ6731 values around 1.2. Our data (cf. Table 2) also show weak [S II] emission (Hα/[S II] = 3.15), and a λ6717/λ6731 ratio of 1.4. Judging from its relatively weak [S II], as well as weak [O III], [O I], and [N II] emissions, the spectrum of OA 184 optically resembles that of an H II region more than that of an SNR. Daltabuit, D'Odorico, and Sabbadin (1976) suggested that this might be due partially to OA 184's interaction with neighboring dense interstellar clouds. However, similar [S II] densities have been observed in other remnants (e.g., IC 443) without leading to such peculiar spectral properties. Alternately, Binette *et al.* (1982) suggested that H II region emission may contaminate OA 184's optical regions. Yet, none of OA 184's emission regions show strong [S II] or [O III] emission typical of remnants (see photographs in Parker, Gull, and Kirshner 1979). It is therefore puzzling that there is such a close positional agreement between the H II region type of optical emission regions and the brightest nonthermal radio contours (Willis 1973). OA 184 is one of the largest optically detected remnants, with an estimated diameter of between 60 and 95 pc (Caswell and Lerche 1979; Milne 1979).

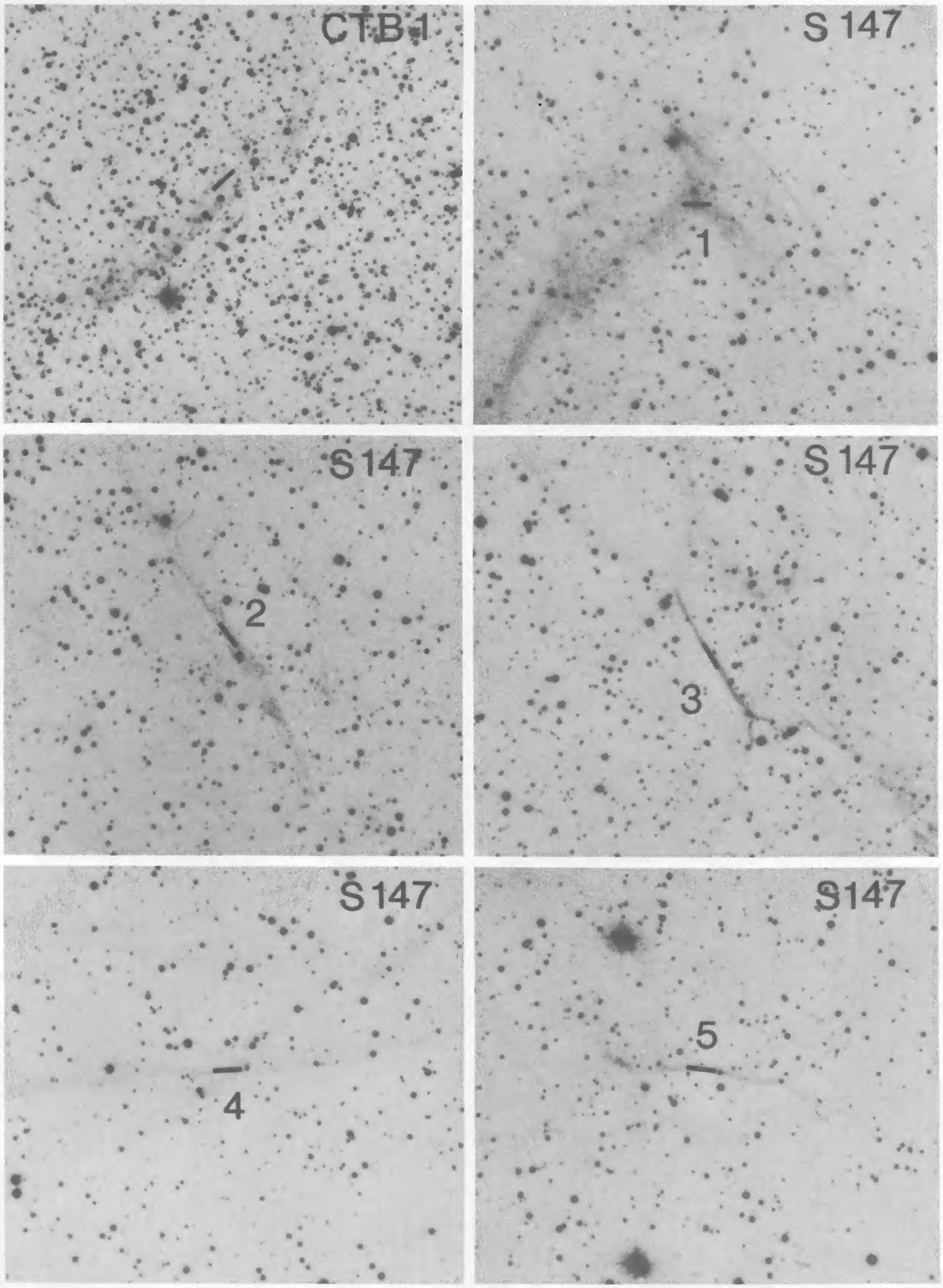

FIG. 1.—Enlargements of the Palomar Observatory Sky Survey E prints showing slit positions in the seven supernova remnants studied. Each finder field is approximately 10′ × 12′.

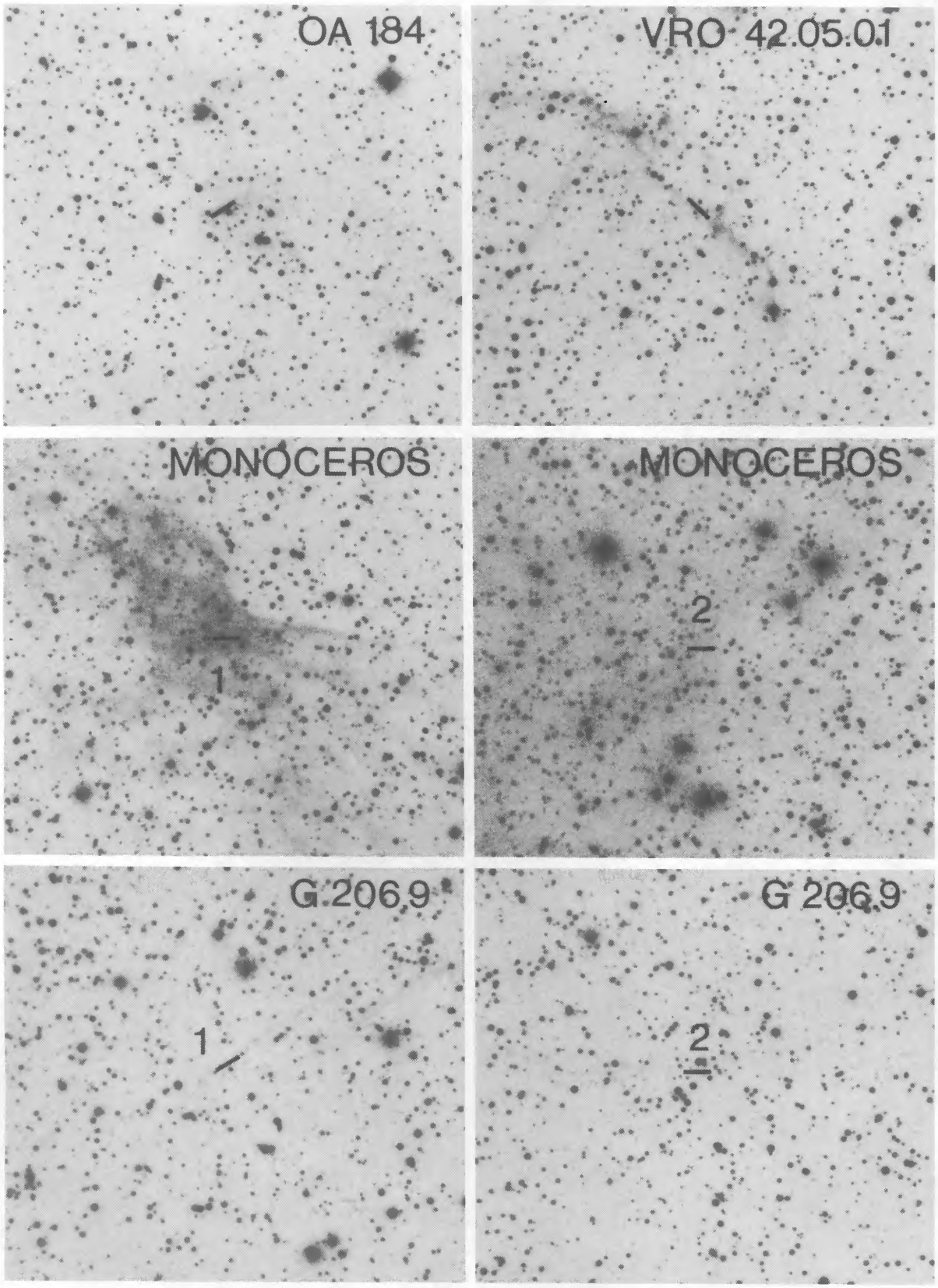

FIG. 1.—*Continued*

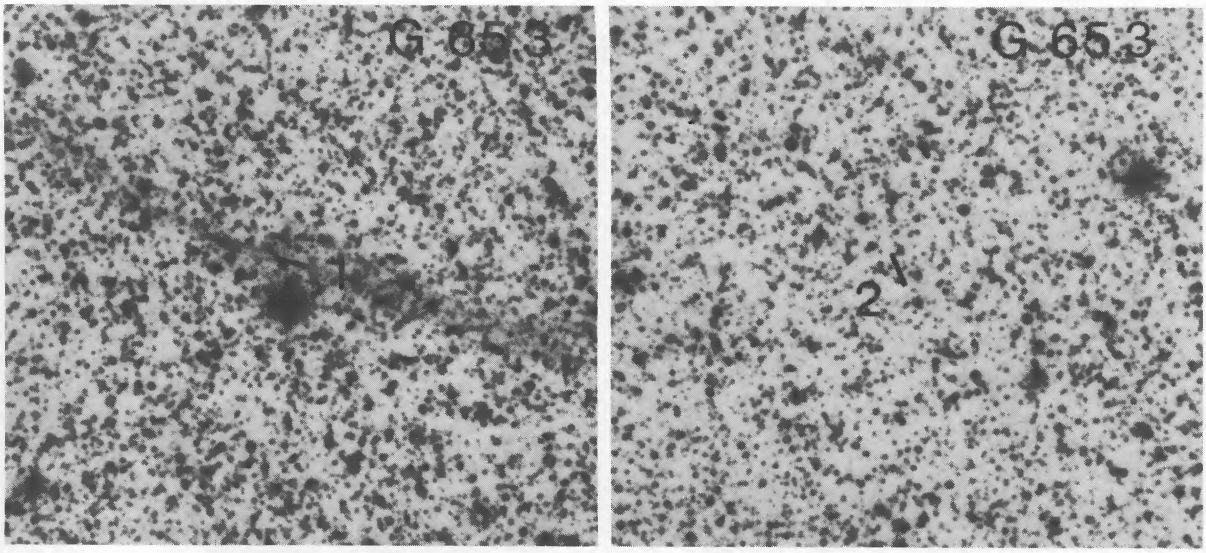

FIG. 1.—*Continued*

c) *VRO 42.05.01 (G166.0+4.3)*

Optical spectra of this remnant were first obtained by Esipov *et al.* (1972), who reported large line intensity variations among its filaments. Although D'Odorico and Sabbadin (1977) found only small changes in line emission strengths at six positions in both northern and southern filaments, interference-filter photographs do suggest substantial [O III]/Hα ratio variations throughout the remnant (Fesen, Gull, and Ketelsen 1983). Recent radio studies show that this remnant possesses a highly asymmetrical structure, possibly because of density variations in the remnant's ambient interstellar medium (Landecker *et al.* 1982). Our single spectrum was obtained on a bright northern filament near D'Odorico and Sabbadin's (1977) position 4, and shows line ratios different from D'Odorico and Sabbadin's values. Whereas they report an Hα/[N II] of 1.48 and an Hα/[S II] of 1.15, we observe 1.75 and 1.45, respectively. Although it is not possible from our data to measure reliably the individual 6717 and 6731 Å [S II] line intensities, the profile of the 6725 Å blend indicates a ratio near the low-density limit of 1.4, which would be consistent with D'Odorico and Sabbadin's measurements.

d) *S147 (G180.0−1.7)*

Previous spectroscopic studies of S147 by Parker (1964), Esipov *et al.* (1972), and D'Odorico and Sabbadin (1977) indicated line intensity ratios for Hα/[S II] between 0.7 and 0.9 and for Hα/[N II] between 1.20 and 1.58. Kirshner and Arnold (1979) reported qualitative relative density estimates for 23 filaments using both the [O II] and the [S II] doublet lines, and found systematic density differences between diffuse and crisp appearing filaments. From our spectroscopy of five positions, we find values for Hα/[S II] of 0.89–1.08 and for Hα/[N II] of 1.05–1.44. The spectrum for position 3 indicates an electron temperature estimate for [O III] of 52,000 ± 10,000 K and a temperature for [N II] of 12,000 ± 3000 K. In this as well as the other four filament positions studied, the [S II] λ6717/λ6731 ratio was observed near the low-density limit of 1.4. Therefore, assuming a density of 100 cm^{-3}, we estimate an electron temperature for [S II] of 9500 ± 2000 K and a temperature for [O II] of 17,500 ± 3500 K for filament 3. With observed Hα/Hβ ratios near 3.75, the interstellar reddening to S147 appears fairly small, with $A_V \sim 0.7$ mag. This is consistent with general galactic reddening values at its estimated ~1 kpc distance using the Σ-*D* relation (Reich, Berkhuijsen, and Sofue 1979).

e) *The Monoceros Loop (G205.6−0.1)*

D'Odorico and Sabbadin (1977) obtained red spectra of two locations in this remnant; one near an apparent reflection nebula around the star HD 46300, and the other of a filament in this remnant's northern section. However, the spectrum taken near the suspected reflection nebula showed stronger [S II] emission (Hα/[S II] = 1.15) than that of the northern filament (Hα/[S II] = 2.15).

We also studied two locations in this SNR. Position 1 examined a relatively bright region of filaments near the Loop's western rim. Its spectrum shows moderately strong [S II] emission (Hα/[S II] = 1.40) but relatively weak [O III] and [O I] emission. Position 2, a filament in the southwest, was chosen to test Kirshner, Gull, and Parker's (1978) suggestion that the relatively bright [O III] emission in this area was due to a higher velocity shock. However, position 2's spectrum shows much weaker [S II] emission (Hα/[S II] = 6.1) than is usually observed in SNR spectra. In the absence of [O III] electron temperature information, the weak [S II] emission suggests that this nebulosity is probably that of an H II region and not an SNR.

The [S II] λ6717/λ6731 line intensity ratio of 1.3 for position 1 is similar to that found by D'Odorico and Sabbadin (1977). The remnant's weak [O III] emission suggests a shock velocity <90 km s^{-1} (Raymond 1979), consistent with Lozinskaya's (1972) expansion velocity measurements of 45 km s^{-1}. Our spectral data also indicate a difference of extinction between the two positions observed, with positions 1 and 2 exhibiting $A_V = 0.94$ and 0.40 mag, respectively. Reddening variations across the face of this remnant are not surprising considering the dust lanes visible in this direction (Davies *et al.* 1978). It is interesting to note, however, that both of these extinction values are considerably lower than those estimated for the

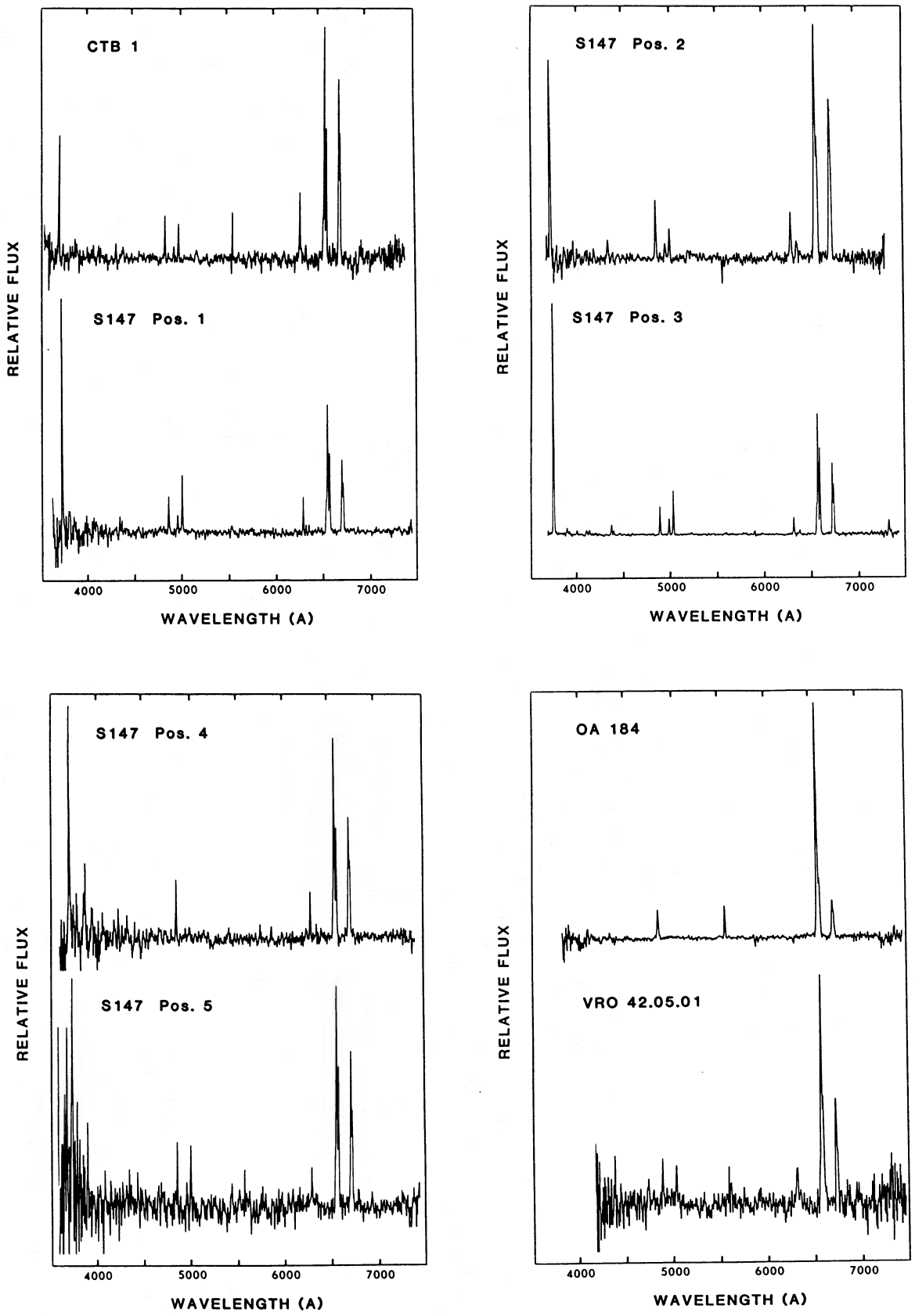

FIG. 2.—Spectra for each remnant position observed. Relative flux, ergs cm^{-2} s^{-1} $Å^{-1}$, is plotted vs. observed wavelength. The feature in some spectra at 5577 Å is residual night sky [O I] emission due to imperfect sky subtraction.

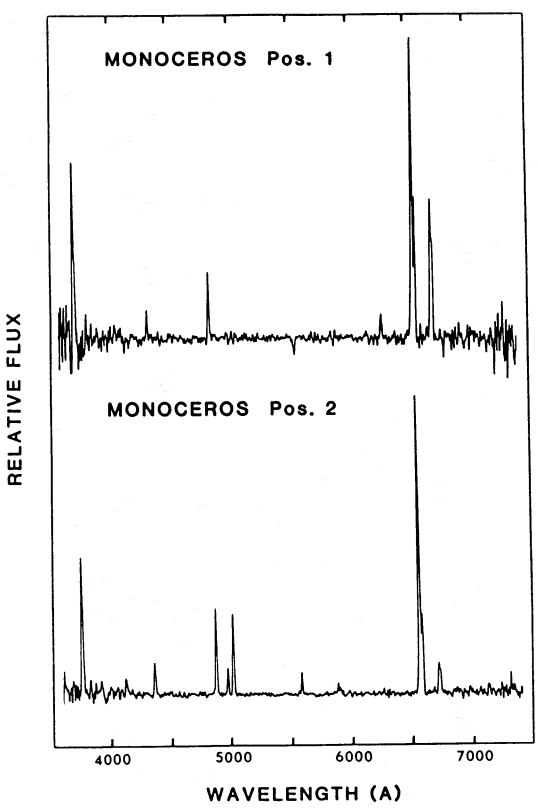

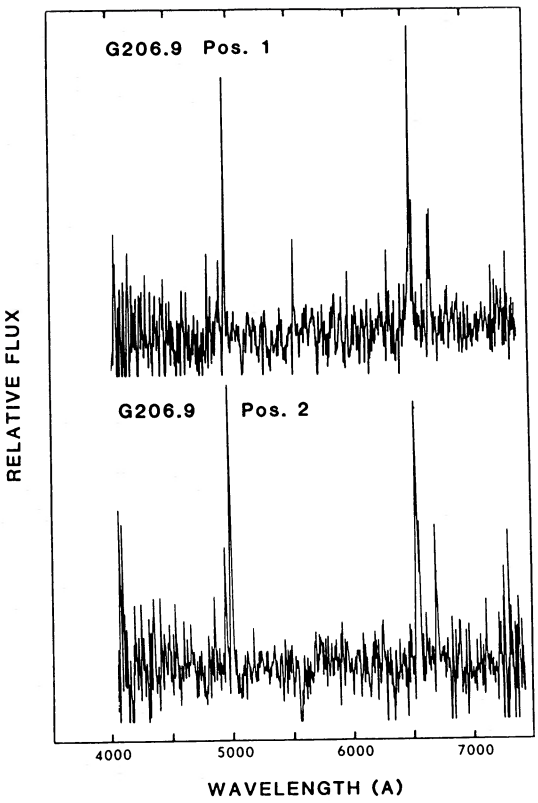

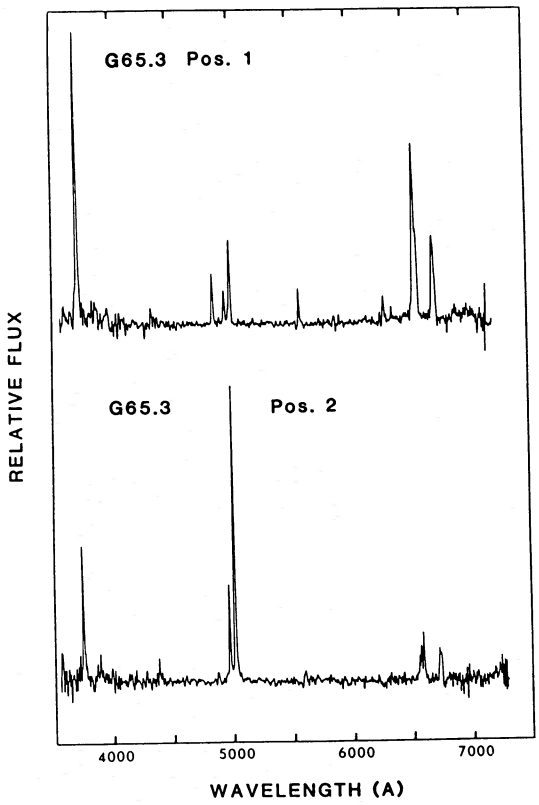

FIG. 2.—*Continued*

TABLE 2

LINE INTENSITIES

							Monoceros Loop				G206.9+2.3				G65.3+5.7			
	CTB 1		OA 184		VRO 42.05.01		Position 1		Position 2		Position 1		Position 2		Position 1		Position 2	
IDENTIFICATION	$F(\lambda)$	$I(\lambda)$	$F(\lambda)$	$I(\lambda)$	$F(\lambda)$	$I(\lambda)$	$F(\lambda)$	$I(\lambda)$	$F(\lambda)$	$I(\lambda)$	$F(\lambda)$	$I(\lambda)$	$F(\lambda)$	$I(\lambda)$	$F(\lambda)$	$I(\lambda)$	$F(\lambda)$	$I(\lambda)$
[O II] λ3727 ...	3.15	5.21	...	...	...	...	2.62	3.50	1.60	1.81	...	...	...	...	5.66	6.31	12.8	13.5
Hδ λ4102	...	...	...	...	...	...	...	...	0.18	0.20	...	...	...	...	...	...	...	...
Hγ λ4340	...	...	0.33	0.44	...	...	0.44	0.51	0.39	0.42	...	...	...	...	(0.39)	(0.41)	...	...
[O III] λ4363 ..	...	...	...	...	...	...	...	...	...	...	...	...	...	...	...	...	2.17	2.23
Hβ λ4861	1.00	1.00	1.00	1.00	1.00	1.00	1.00	1.00	1.00	1.00	1.00	1.00	1.00	1.00	1.00	1.00	(1.00)	(1.00)
[O III] λ4959 ..	0.29	0.28	...	...	...	...	...	...	0.29	0.29	0.95	0.93	1.65	1.62	0.65	0.64	9.31	9.26
[O III] λ5007 ..	0.79	0.74	(0.15)	(0.14)	0.95	0.91	(0.10)	(0.10)	0.94	0.93	3.12	3.04	4.09	4.00	1.66	1.63	29.0	28.8
[N I] λ5199	(0.15)	(0.13)	...	...	...	...	...	...	...	...	...	...	...	...	0.09	0.09	...	...
[O I] λ6300	(1.30)	(0.77)	<0.25	<0.14	0.96	0.66	(0.30)	(0.24)	<0.15	<0.13	<1.00	<0.82	...	...	(0.50)	(0.45)	<1.00	<0.95
[O I] λ6364	(0.45)	(0.26)	...	...	...	...	...	...	...	...	...	...	...	...	(0.19)	(0.17)	...	...
[N II] λ6548 ...	1.08	0.60	...	...	(0.70)	(0.39)	0.88	0.63	0.25	0.22	0.75	0.59	...	...	...	...	(1.85)	(1.74)
Hα λ6563	5.40	3.00	5.86	3.00	5.46	3.00	4.20	3.00	3.46	3.00	3.79	3.00	3.62	3.00	3.40	3.00	(3.20)	(3.00)
[N II] λ6583 ...	3.05	1.69	1.50	0.76	2.62	1.43	1.92	1.37	0.87	0.75	2.00	1.58	2.11	1.74	1.73	1.52	4.57	4.28
[S II] λ6717	3.91	2.09	1.05	0.52	4.02	2.12	1.85	1.29	0.33	0.28	1.75	1.36	2.38	1.95	1.55	1.36	3.05	2.85
[S II] λ6731	2.94	1.57	0.89	0.43			1.31	0.92	0.25	0.21	1.65	1.28			1.20	1.05	2.74	2.54
A_V (mag)	1.64		1.86		1.68		0.94		0.40		0.65		0.52		0.35		(0.18)	

TABLE 2—*Continued*

	S147									
	Position 1		Position 2		Position 3		Position 4		Position 5	
IDENTIFICATION	$F(\lambda)$	$I(\lambda)$	$F(\lambda)$	$I(\lambda)$	$F(\lambda)$	$I(\lambda)$	$F(\lambda)$	$I(\lambda)$	$F(\lambda)$	$I(\lambda)$
[O II] λ3727	6.15	7.15	3.78	4.88	8.50	11.2	4.24	5.41	(3.54)	(4.27)
[Ne III] λ3867	...	...	...	...	0.22	0.28	...	...	...	...
He + H λ3888	...	...	...	...	0.08	0.10	...	...	...	...
[Ne III] + H λ3970	...	...	...	...	0.14	0.17	...	...	...	...
[S II] λ4072	...	...	...	...	0.15	0.18	...	...	...	...
Hδ λ4102	...	...	...	...	0.16	0.19	...	...	...	...
Hγ λ4340	0.43	0.47	0.33	0.38	0.33	0.38	...	...	...	...
[O III] λ4363	...	...	...	...	0.13	0.15	...	...	...	...
Hβ λ4861	1.00	1.00	1.00	1.00	1.00	1.00	1.00	1.00	1.00	1.00
[O III] λ4959	0.49	0.48	(0.26)	(0.25)	0.55	0.54	...	...	(0.33)	(0.35)
[O III] λ5007	1.60	1.57	0.51	0.49	1.55	1.50	(0.23)	(0.22)	0.94	0.91
[N I] λ5199	...	...	...	...	0.07	0.06	...	...	...	...
[N II] λ5755	...	...	...	...	(0.06)	(0.05)	...	...	...	...
He I λ5876	...	...	...	...	0.13	0.11	...	...	...	...
[O I] λ6300	0.92	0.79	0.80	0.62	0.60	0.45	0.79	0.62	0.63	0.53
[O I] λ6364	...	...	0.29	0.22	0.20	0.15	...	...	...	...
[N II] λ6548	0.90	0.76	(0.98)	(0.73)	0.95	0.69	0.81	0.63	(0.47)	(0.39)
Hα λ6563	3.57	3.00	4.03	3.00	4.12	3.00	3.98	3.00	3.73	3.00
[N II] λ6583	2.22	1.86	2.15	1.60	2.87	2.08	2.13	1.61	2.12	1.70
He I λ6678	...	...	...	...	0.05	0.04	...	...	...	...
[S II] λ6717	2.06	1.71	2.73	1.99	2.36	1.68	2.35	1.76	2.62	2.10
[S II] λ6731	1.35	1.12	1.85	1.35	1.67	1.19	1.55	1.14	1.42	1.13
[Ar III] λ7135	...	...	...	...	0.09	0.06	...	...	...	...
[O II] λ7325	...	...	...	...	0.64	0.42	...	...	...	...
A_V (mag)	0.48		0.82		0.88		0.79		0.61	

NOTE.—Parentheses denote significantly more uncertain values.

TABLE 3

IMPLIED DISTANCES FROM OBSERVED REDDENING

Remnant	A_V	Reddening-implied Distance (kpc)	Σ-D[a] Relation Distance (kpc)
CTB 1	1.64	>1.0	4.7
OA 184	1.86	~2.0	2.2
VRO 42.05.01	1.68	>2.0	3.6
S147	0.70	~0.8	0.9
Monoceros Loop	0.94	~ 1.0	0.7
G206.9+2.3	0.59	<1.0	2.3[b]
G65.3+5.7	0.35	<1.0	0.9

[a] Clark and Caswell 1976.
[b] Reich, Berkhuijsen, and Sofue 1979.

neighboring Rosette nebula (NGC 2244; $A_V = 2.2$) or for NGC 2264 ($A_V = 4.0$) (Kaler 1976) for which interactions with this remnant have been proposed (Davies *et al.* 1978; Kirshner, Gull, and Parker 1978).

f) G206.9+2.3 (PKS 0646+06)

Two thin filaments in this remnant's northeastern and southern sections observed by us are the first spectra reported for this remnant. The λ6717/λ6731 line intensity ratio of 1.1 for position 1 implies a fairly high density of 800 cm^{-3}, but no density estimate is possible from our data for position 2. While our data at position 2 indicate modest [O III] emission, i.e., [O III]/Hβ ~ 4–6, both Rosado (1982) and T. Gull (1981, private communication) report interference-filter images of this object which suggest that some filaments may have very large [O III]/Hβ ratios. The observed Hα/Hβ ratio implies an $A_V = 0.6 \pm 0.25$ mag. Unless located in a direction of relatively low extinction compared with neighboring regions, this value implies a distance of <1 kpc, which is substantially less than the value of 2.3 kpc estimated from its radio properties (Clark and Caswell 1976).

g) G65.3+5.7 (S91+S94)

Van den Bergh (1960) suggested that two filamentary nebulae, S91 and S94 (Sharpless 1959) were probably associated with an SNR. Clear evidence for the existence of this remnant came from Gull, Kirshner, and Parker (1977), who obtained an [O III] interference-filter photograph of the region revealing a nearly complete 3°.3 × 4°.0 filamentary shell. High-resolution imagery of several selected regions of this remnant are discussed by Rosado (1981), Fesen, Gull, and Ketelsen (1983), and Sitnik, Klement'eva, and Toropova (1983).

Up to now, optical spectroscopy of this remnant was limited to the red spectra of Sabbadin and D'Odorico (1976) for three regions in the S91 filaments. Their results gave average Hα/[N II] and Hα/[S II] ratios of 1.04 and 0.93, respectively, with a λ6717/λ6731 ratio of 1.30. We obtained spectra at two regions, one in S91 (position 1) close to Sabbadin and D'Odorico's locations, with position 2 on one of the remnant's brightest [O III] filaments (see Fig. 2 in Fesen, Gull, and Ketelsen 1983). At position 1, our Hα/[N II] and Hα/[S II] ratios of 1.5 and 1.3 are larger than those reported by Sabbadin and D'Odorico, while the λ6717/λ6731 value of 1.30 is nearly identical with theirs. Although the spectrum of S91's filaments appears similar to those observed in other SNRs, that of position 2

shows an especially large [O III]/Hβ ratio. The Hβ intensity could not be measured with high accuracy, but the data suggest an [O III]/Hβ ratio of about 40. While this is about twice as large as is usually observed for strong [O III] regions in other remnants, judging from interference-filter photographs, this may be typical for many of this remnent's filaments. However, the [O III] electron temperature for position 2 estimated from its 4363 Å line strength is not unusually large at 38,000 $\pm$ 7000 K. This filament also exhibits relatively strong [N II] and [S II] emissions, with Hα/[N II] = 0.50 and Hα/[S II] = 0.56.

IV. DISCUSSION

In order to study general spectral properties of evolved galactic supernova remnants, it is important to exclude from consideration young remnants which may be dominated by supernova ejecta, as well as very peculiar remnants. The photoionized and helium-rich Crab Nebula (Davidson 1979; Henry and MacAlpine 1982; Péquignot and Dennefeld 1983) and the oxygen- and sulfur-rich fast-moving knots of Cas A (Kirshner and Chevalier 1977; Chevalier and Kirshner 1979) have considerably different spectral properties from those seen in evolved remnants like the Cygnus and Monoceros loops, whose emissions arise from shocked interstellar clouds. It would therefore be inappropriate to group such different remnants together and draw general conclusions about systematic spectral evolutionary or abundance variations based only upon differences of line-emission strengths. Nevertheless, some previous investigations of SNR line emissions have not made such distinctions (Daltabuit, D'Odorico, and Sabbadin 1976; D'Odorico and Sabbadin 1976; Sabbadin 1977; Dopita 1977). We will thus restrict our discussion to only evolved remnants whose optical emission appears due to shock heating of the remnant's local interstellar medium. Such remnants should then have related though not identical spectral properties.

Remnants therefore excluded from our discussion are the young remnants associated with historically observed supernovae as well as SNRs exhibiting either an unusual morphology or peculiar line strengths suggestive of some supernova or presupernova element enrichment. The remnants omitted are Cas A, Kepler's SNR, Tycho's SNR, the Crab Nebula, 3C 58 (SN 1181), SN 1006, G292.0+1.8, and Puppis A. While RCW 86 has been suggested as being the remnant of SN 185 (Clark and Stephenson 1977), it does not exhibit any marked peculiarities in its spectrum (Ruiz 1981). With an estimated radius of $\sim$15 pc and assuming an average interstellar medium density of 1 cm^{-3}, RCW 86 could have swept up 300 $M_\odot$ of interstellar mass, thereby substantially diluting the SN ejecta; hence it will be included in our sample. The remnants RCW 89 and RCW 103 are unusual in that they appear relatively evolved yet have associated X-ray point sources (Tuohy and Garmire 1980; Seward *et al.* 1983). However, since they do show normal shell structures, they too will be included in our sample. On the other hand, CTB 80, because of its extremely peculiar morphology and low expansion velocities (cf. Angerhofer, Wilson, and Mould 1980; Blair *et al.* 1984), along with the remnants G109.1$-$1.0 (because of its bright central X-ray pulsar) and W50 (associated with SS 433), will be omitted. Finally, because of its atypically weak [S II], [N II], [O I], and [O III] line emissions, the remnant OA 184 will also be excluded from our discussion. The remaining SNRs for which optical spectroscopy is available are listed in Table 4, along with the references to the optical data used. A similar group of remnants has been used by Binette *et al.* (1982) to study the galactic abundance gradient, with the difference that we have omitted W50, OA 184, and 3C 58 for the reasons given above, and G296.5+10.0 (because of a lack of accurate spectral data), while including our new spectral data on seven remnants. Below we discuss spectral identification criteria for distinguishing remnants from other emission-line nebulae and the observed range of relative line strength variations present within individual objects, and we examine galactic abundance gradients and evolutionary emission-line trends.

a) Emission-Line Criteria for SNR Identification

Spectroscopically, SNRs can generally be characterized by strong forbidden line emission exhibiting a wide range of ionization states. For example, in contrast to H II regions or planetary nebulae, the optical forbidden oxygen lines [O I] $\lambda\lambda$6300, 6364, [O II] λ3727, and [O III] $\lambda\lambda$4959, 5007 are often simultaneously strong in remnants. However, the most generally used quantitative criterion for distinguishing SNRs from H II regions has been the stronger [S II] $\lambda\lambda$6717, 6731 emission of SNRs, i.e., Hα/[S II] < 2.0. The presence of electron temperatures $\sim$10,000 K in the S^+ zone of the nonequilibrium recombination shock region of a remnant together with the large collisional cross sections of these [S II] transitions leads to stronger [S II] emission than is usually observed in photoionized H II regions (or planetary nebulae), where the sulfur is usually in the form of S^{++}. Strong [S II] emission has proved an enormously useful yet simple tool in optically identifying both galactic and extragalactic SNRs (Mathewson and Clarke 1972, 1973; van den Bergh 1978; D'Odorico, Dopita, and Benvenuti 1980; Blair, Kirshner, and Chevalier 1981).

The Hα/[S II] criterion has some drawbacks, however. The lowest observed Hα/[S II] ratios in H II regions and low-excitation planetary nebulae are nearly the same as the largest values seen in some remnants. This has led to some ambiguity in the identification of some objects (e.g., S216; Fesen, Blair, and Gull 1981), as well as causing some confusion about what specific value to use in order to separate SNRs from H II regions. Mathewson and Clarke (1973) chose a value around 1.5, Daltabuit, D'Odorico, and Sabbadin (1976) a value of $\sim$ 2.0, while D'Odorico (1978) suggests a value of about 2.5. Therefore, in borderline cases, another emission-line ratio criterion would clearly be valuable.

To be a useful discriminator, the emission lines considered should be readily observable and not greatly affected by other factors such as temperature and abundance. Although values of less than 30 for the electron temperature–sensitive line ratio of [O III] (λ4959 + λ5007)/λ4363 are always observed in SNRs (i.e., $T_e > 20{,}000$ K) but are never seen even for the hottest H II regions and planetary nebulae, the 4363 Å line is usually too weak and the sky Hg I λ4358 line often too strong to permit its use as a general remnant diagnostic. Likewise, the [S II]/[Ar III] ratio discussed by Boeshaar *et al.* (1980) is limited in its applicability by the faintness of the [Ar III] λ7136 line in SNRs. While most galactic remnants exhibit Hα/[N II] values less than about 3, the nitrogen lines vary considerably as a function of nitrogen abundance, thus changing from galaxy to galaxy as well as within a galaxy if an abundance gradient is present (cf. Shaver *et al.* 1983). A more practical criterion could be based upon [O I] and [O II] line strengths in those cases where good sky [O I] subtraction is possible (Fesen 1981; Blair, Kirshner, and Chevalier 1982). Remnant [O I]/Hβ and [O II]/Hβ ratios are almost always observed to be much larger than those for

TABLE 4

EVOLVED GALACTIC SUPERNOVA REMNANTS WITH MEASURED OPTICAL SPECTRA

REMNANT	AVERAGE VALUE		CLARK AND CASWELL 1976		SPECTRAL DATA REFERENCES
	[N II]/Hα	6717/6731	Diameter (pc)	Galactocentric Distance (kpc)	
W28	1.09	1.03	32	7.7	1
3C 400.2	1.19	1.20	41	8.1	2
G65.3+5.7	0.79	1.30	(75)[a]	(9.6)[a]	2, 3
Cygnus Loop	1.09	1.27	44	9.8	4, 5
W63	0.65	1.30	38	9.9	6
CTB 1	0.68	1.33	(21)[b]	(11.1)[b]	3, 7
CTA 1	1.15	1.27	49	10.7	8
G126.2+1.6	0.97	1.33	(89)[c]	(13.1)[c]	9
HB 3	0.49	1.44	41	11.4	7
HB 9	0.75	1.33	43	11.0	7
VRO 42.05.01	0.56	1.36	46	13.5	3, 7
S147	0.74	1.40	48	10.9	3, 7
IC 443	0.78	1.26	(22)[d]	(11.6)[d]	5, 10
G206.9+2.3	0.74	1.12	54	12.1	3
Monoceros Loop	0.70	1.37	49	10.6	3, 7
Vela	1.12	1.21	38	10.1	1, 11
G290.1−0.8	0.60	1.20	21	9.7	12
G296.1−0.7	1.25	1.23	39	9.8	13
Centaurus	1.00	1.15	42	9.3	14
RCW 86	1.12	0.80	36	8.1	15, 16
RCW 89	1.79	0.89	33	7.2	1
RCW 103	2.22	0.78	24	4.6	15
MSH 15−56	1.47	1.17	33	7.6	17

[a] Diameter = 75 pc, distance = 0.9 kpc (Reich, Berkhuijsen, and Sofue 1979).
[b] Diameter = 21 pc, distance = 2.0 kpc (Landecker, Roger, and Dewdney 1982).
[c] Diameter = 89 pc, distance = 4.6 kpc (Reich, Kallas, and Steube 1979).
[d] Assumed distance of 1.5 kpc (Fesen 1984).

REFERENCES.—(1) Dopita, Mathewson, and Ford 1977. (2) Sabbadin and D'Odorico 1976. (3) This work. (4) Osterbrock 1958; Parker 1967; Miller 1974; Fesen, Blair, and Kirshner 1982. (5) Parker 1964. (6) Sabbadin 1976. (7) D'Odorico and Sabbadin 1976. (8) Fesen *et al.* 1981. (9) Blair *et al.* 1980. (10) D'Odorico 1974; Fesen and Kirshner 1980. (11) Osterbrock and Costero 1973. (12) Elliott and Malin 1979. (13) Longmore, Clark, and Murdin 1977. (14) Danziger and Dennefeld 1976. (15) Dopita, D'Odorico, and Benvenuti (1980); Leibowitz and Danziger 1983. (16) Ruiz 1981. (17) Dennefeld 1980.

H II regions. Although this has been realized for some time (see Baldwin, Phillips, and Terlevich 1981), a treatment using recent galactic remnant data has not been presented.

The ability of the [O I]/Hβ and [O II]/Hβ line ratios to separate SNRs from H II regions is shown in Figure 3, where reddening-corrected values for [O II] λ3727 are plotted against [O I] λλ6300, 6364 for our list of remnants in Table 4. In order to suppress measurement errors due to the fainter [O I] λ6364 line, we have taken $I(6364) \equiv \frac{1}{3} \times I(6300)$. The data plotted are for the Cygnus Loop (Miller 1974; Fesen, Blair, and Kirshner 1982), RCW 86 (Dopita, D'Odorico, and Benvenuti 1980; Ruiz 1981), RCW 103 (Dopita, D'Odorico, and Benvenuti 1980; Leibowitz and Danziger 1983), IC 443 (Fesen and Kirshner 1980), Vela X (Osterbrock and Costero 1973), and S147, CTB 1, the Monoceros Loop, and G65.3+5.7 from this work. The H II region data were taken from Kaler (1976), Peimbert and Torres-Peimbert (1977), Peimbert, Torres-Peimbert, and Rayo (1978), Hawley (1978), and Talent and Dufour (1979). When no value for [O I] line strength is given for an H II region, we assumed that its I([O I] λ6300) value must be less than I([S III] λ6312), which was reported and measured. Where multiple positions were observed, the strongest [O I]/Hβ and [O II]/Hβ emitting position for the H II region is listed. Thus, in general, the separation between remnants and H II regions should be

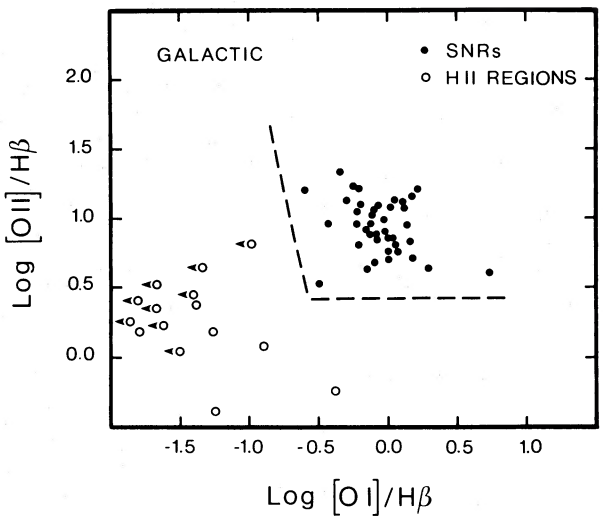

FIG. 3.—Extinction-corrected log ([O II]/Hβ) vs. log ([O I]/Hβ) for galactic supernova remnants (*dots*) and H II regions (*open circles*). The dashed line indicates the limit of observed ratio values for remnants. The figure illustrates the considerable difference for these emission-line ratios between remnants and H II regions.

larger than indicated in this figure. That is to say, a significant fraction of galactic H II regions not shown here would occupy the far lower left-hand portion of the figure, having log ([O I]/Hβ) < −1.2 and log ([O II]/Hβ) < 0.6 (e.g., see Orion values in Peimbert and Torres-Peimbert 1977). In contrast, SNRs exhibit considerably larger values for both line ratios. The figure shows a clear and definite segregation of SNRs from H II regions with no apparent overlap. While a single remnant's in Peimbert and Torres-Peimbert 1977). In contrast, SNRs exhibit considerably larger values for both line ratios. The figure shows a clear and definite segregation of SNRs from H II regions with no apparent overlap. While a single remnant's filaments may scatter widely within the SNR region of the figure, even for an extreme range of filament characteristics the values still all fall within the remnant region (e.g., the Cygnus Loop data; Fesen, Blair, and Kirshner 1982). Although about 40% of the data comes from the Cygnus Loop alone, the other points represent 25 filaments in eight other remnants. (Note: similar differences for these ratios usually exist between planetary nebulae and SNRs as well [cf. Barker 1978], but there are clear exceptions [cf. Hawley and Miller 1977; Kwitter, Jacoby, and Lawrie 1983]).

In cases where remnant identification is uncertain via the Hα/[S II] ratio (i.e., values near 2), the [O I] and [O II] lines could prove most useful. Since the change of the [O I] emission between SNRs and H II regions is greater than for the [S II] lines, [O I] is a more sensitive shock emission test and is particularly good where there is suspicion of contamination of remnant spectra by H II region emission. For example, since the optical emission believed associated with the remnant OA 184 shows no detectable [O I] emission, it is probably just that of an H II region and not faint remnant emission contaminated by an H II region.

The generality of the [O I] versus [O II] relation is illustrated in Figure 4, which shows the observed ratios for the SNRs and H II regions in M31 and M33 (Dopita, D'Odorico, and Benvenuti 1980; Blair, Kirshner, and Chevalier 1981, 1982; Dennefeld and Kunth 1981; Blair and Kirshner 1985). Again, a clear separation of remnants and H II regions is apparent at about the same values as for the galactic remnants. As noted by Blair, Kirshner, and Chevalier (1982), the M31 objects BA 337 and BA 370 (indicated in Fig. 4 by asterisks), though exhibiting only modest [S II] emission, can be identified as remnants on the basis of their [O I] and [O II] line strengths. However, this [O I]:[O II] criterion is most effective when used in concert with the Hα/[S II] ratio test. For example, the filamentary shell N70 in the LMC has very strong [O I] and [O II] emission but relatively weak [S II] emission and low [O III] temperatures and is probably not an SNR (Dopita *et al.* 1981). Therefore, [O I] and [O II] line strengths, when used *in conjunction* with the Hα/[S II] ratio, are an effective tool for helping to identify galactic and extragalactic SNRs.

b) *Line Strength Variations within Individual SNRs*

Although the strengths of some lines such as [O I], [O II], and [O III] relative to Hβ have been observed to vary significantly within an individual remnant (see Fesen, Blair, and Kirshner 1982), it is useful to establish the corresponding range of variations for Hα/[N II] and Hα/[S II], as well as the density-sensitive [S II] λ6717/λ6731 ratio. Daltabuit, D'Odorico, and Sabbadin (1976) suggested that these intensity ratios change less from point to point within a remnant than they do between different remnants. They used this principle to develop an evolutionary scheme in which the Hα/[N II] and λ6717/λ6731 ratios vary systematically as a function of remnant diameter as estimated from the Σ-D relationship. Since many galactic remnants have had only a few of their filaments studied spectroscopically, large variations among a single remnant's filaments might affect such proposed evolutionary trends. More important, the Hα/[N II] and Hα/[S II] ratios have been used to infer abundance gradients in the Milky Way, M31, and M33 (Dopita, D'Odorico, and Benvenuti 1980; Blair, Kirshner, and Chevalier 1981, 1982; Binette *et al.* 1982; Blair and Kirshner 1985). Large variations of these ratios within individual remnants could affect the accuracy of gradients derived in this way.

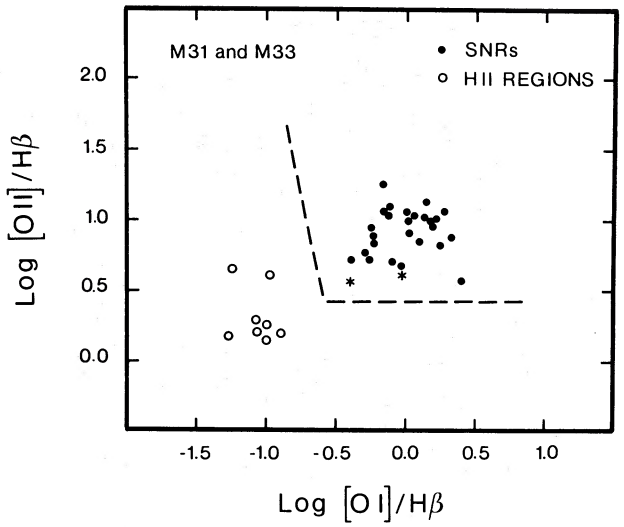

FIG. 4.—Same as Fig. 3, but for M31 and M33 remnants and H II regions. The two M31 remnants with relatively weak [S II] emission (BA 337 and BA 370) are indicated by asterisks.

To investigate the ranges of observed line ratios within and between remnants, we list in Table 5 the data on these ratios for our sample of evolved remnants having three or more filaments observed. Because of differences among observers (e.g., instruments, spectral resolution, apertures, signal-to-noise ratios, etc.), each set of values is listed separately. The table gives the range of observed ratios, mean values, and percent standard deviations from the mean.

These data indicate that within a single remnant, even with measurement errors considered which are typically 5%–25%, relatively small variations in the observed *mean* values are the rule for these ratios. While differences exist between mean values among different observers, the dispersion in each data set is small. This suggests an intrinsically small scatter within individual objects. The Cygnus Loop data are particularly valuable in this regard, because of the number of filaments studied, the relatively small measurement errors (5%–10%), and the wide variety of filament spectra observed. The filaments observed in the Cygnus Loop by Fesen, Blair, and Kirshner (1982) were in fact specifically chosen to investigate the range of line-ratio variations present within that remnant. The relatively modest differences reported for the mean values of these emission lines among the Cygnus Loop's filaments support Dopita *et al.*'s (1984) suggestion that these lines are primarily sensitive to chemical abundances rather than shock conditions. From Table 5 we estimate a remnant's intrinsic spread to be approximately ±10% for [S II] λ6717/λ6731, ±20% for Hα/[N II], and ±30% for Hα/[S II]. Similar scale

TABLE 5

LINE INTENSITY VARIATIONS IN GALACTIC SUPERNOVA REMNANTS

REMNANT	NUMBER OF OBSERVATIONS	Hα/[N II]			Hα/[S II]			[S II] λ6717/λ6731			REFERENCES
		Range	Mean	% Std	Range	Mean	% Std	Range	Mean	% Std	
IC 443	19	1.04–1.50	1.28	±14%	0.55–0.89	0.72	±14%	1.09–1.75	1.30	±16%	Parker 1964
IC 443	28	0.90–1.70	1.27	±19%	0.60–1.07	0.77	±15%	0.95–1.41	1.22	±9%	D'Odorico 1974
IC 443	6	1.15–1.49	1.32	±9%	0.87–1.09	0.95	±10%	1.10–1.53	1.31	±12%	Fesen and Kirshner 1980
Cygnus Loop	7	...	...	...	...	...	...	1.20–1.47	1.30	±9%	Osterbrock 1958
Cygnus Loop	18	0.71–1.17	0.90	±14%	0.61–1.56	1.00	±28%	1.01–1.51	1.26	±12%	Parker 1964
Cygnus Loop	9	0.66–1.25	0.90	±17%	0.81–1.49	1.08	±33%	1.00–1.31	1.19	±9%	Parker 1967
Cygnus Loop	3	0.86–0.89	0.88	...	0.79–1.28	1.05	±23%	1.14–1.31	1.21	±7%	Miller 1974
Cygnus Loop	12	0.76–1.25	0.99	±20%	0.77–1.76	1.06	±26%	1.27–1.51	1.40	±6%	Fesen, Blair, and Kirshner 1982
S147	6	1.20–1.58	1.44	±9%	0.71–0.92	0.79	±10%	1.27–1.44	1.35	±6%	D'Odorico and Sabbadin 1976
S147	5	1.08–1.41	1.28	±11%	0.90–1.05	1.00	±8%	1.44–1.85	1.61	±12%	this work
RCW 86	7	0.64–1.12	0.82	±16%	0.92–1.45	1.07	±24%	0.78–0.96	0.86	±7%	Ruiz 1981
RCW 86	10	0.77–1.16	0.94	±12%	0.98–2.48	1.61	±39%	0.59–0.88	0.77	±9%	Leibowitz and Danziger 1983
RCW 103	5	0.39–0.51	0.44	±4%	0.93–1.20	1.03	±11%	0.67–0.87	0.76	±7%	Leibowitz and Danziger 1983
HB 9	3	1.26–1.40	1.32	±6%	1.40–2.00	1.72	±18%	1.26–1.40	1.32	±6%	D'Odorico and Sabbadin 1976
VRO 42.05.01	5	1.48–2.00	1.78	±12%	1.01–1.38	1.21	±12%	1.30–1.45	1.38	±5%	D'Odorico and Sabbadin 1976
CTB 1	8	1.40–1.82	1.63	±9%	1.00–1.25	1.13	±9%	1.31–1.44	1.34	±4%	D'Odorico and Sabbadin 1976
G65.3+5.7	3	1.03–1.05	1.04	±1%	0.90–0.95	0.93	±3%	1.25–1.36	1.30	±4%	D'Odorico and Sabbadin 1976

variations for Hα/[N II] and Hα/[S II] are supported by the digital analysis of interference-filter imaging of the Cygnus Loop by Hester, Parker, and Dufour (1983). Although the results inferred from Table 5 are heavily weighted toward the Cygnus Loop and IC 443 data, they are consistent with values observed in other SNRs.

However, variations of these line ratios among the filaments of individual remnants are important in assessing differences among remnants. For example, the ±20% variation in Hα/[N II] is not a great deal smaller than the ±30% difference (i.e., standard deviation) between the mean ratios for the nine remnants listed. Moreover, the *total* spread of observed values in each of the remnants IC 443 and the Cygnus Loop can be 75% or larger. Therefore, for a remnant having only one or two filaments studied, such variations can lead to uncertainties about conclusions drawn from its use in remnant ratio comparisons. (Such uncertainties can be seen to arise easily from the differences in the reported ratio values for some remnants discussed in § III.)

Finally, the relatively small (~10%) variation estimated for the density-sensitive [S II] λ6717/λ6731 line ratio in this sample of remnants suggests a correspondingly small range of filament densities and cloud pressures. The typical observed evolved remnant λ6717/λ6731 line ratio value greater than 1.10 (with the exception of RCW 86, RCW 89, RCW 103, W28, and G296.1−0.7) indicates electron densities less than 300 cm^{-3}. A 10% variation in this line ratio at such low densities implies filament density changes of only about 200 cm^{-3} and therefore typical maximum densities less than about 500 cm^{-3}.

c) *Emission-Line Correlations as a Function of Evolution and Galactocentric Distance*

The Hα/[N II] ratio has been a widely used tool for investigating nitrogen-to-hydrogen abundance variations among SNRs. D'Odorico and Sabbadin (1976) applied this ratio to study the nitrogen abundance differences between galactic and LMC remnants, while D'Odorico, Benvenuti, and Sabbadin (1978), Dopita, D'Odorico, and Benvenuti (1980), Blair, Kirshner, and Chevalier (1981, 1982), and Binette *et al.* (1982) have used it to infer a nitrogen abundance gradient in M31, M33, and our Galaxy. There is evidence from H II region studies for a nitrogen gradient in our Galaxy (Peimbert, Torres-Peimbert, and Rayo 1978; Hawley 1978; Peimbert 1979; Talent and Dufour 1979; Shaver *et al.* 1983) as well as in M31 and M33 (Dopita, D'Odorico, and Benvenuti 1980; Dennefeld and Kunth 1981; Kwitter and Aller 1981; Blair, Kirshner, and Chevalier 1982), and the abundance gradients determined by the two methods are in remarkably good agreement. Since nitrogen is not a major coolant, within a range of shock velocities and preshock densities the Hα/[N II] ratio should be a good indicator of the N/H abundance in the ISM encountered by the shock wave (Dopita 1977; Raymond 1979; Dopita *et al.* 1984). The limited variations in Hα/[N II] values observed within individual remnants (Table 5) permit an estimate of nitrogen abundance differences among remnants.

We show in Figure 5 the average observed [N II]/Hα ratios for our sample of 23 evolved galactic SNRs as a function of galactocentric distance, using Clark and Caswell's (1976) distance estimates with updates (see Table 5). The trend of line ratio with galactocentric distance has been interpreted by several previous studies as an indication for a galactic nitrogen abundance gradient in the sense that larger [N II]/Hα values (i.e., stronger [N II] line emissions) are found toward the galactic center. The observed correlation is a good one, with a correlation coefficient of −0.80 using the Clark and Caswell data. (Note: this does not include line strength measurement errors, which are typically 5%–15%, or uncertainties in galactic distances, which can be substantial. However, no significant difference results if other distance estimates [e.g., those of Milne 1979] are used.) Even excluding the upper three points (i.e., the remnants RCW 89, RCW 103, and MSH 15−56, which exhibit the largest [N II]/Hα values), one still observes an increase of [N II]/Hα with decreasing distance from the galactic center. The effect is seen as roughly a 50% increase (from 0.75 to 1.15) of the [N II]/Hα ratio with decreasing galactic distances of between 12 and 8 kpc. A nitrogen abundance gradient in our Galaxy has been estimated through H II region data by Hawley (1978), Peimbert (1979), Talent and Dufour (1979), and Shaver *et al.* (1983), which indicates similar [N II]/Hα variations. It seems likely, therefore, that a gradient in the interstellar medium's nitrogen abundance observable by means of the Hα/[N II] ratio in both H II regions and SNRs is present in the Galaxy as well as in the M31 and M33 systems.

However, it has been argued by Daltabuit, D'Odorico, and Sabbadin (1976), D'Odorico and Sabbadin (1976), and Sabbadin (1977) that galactic remnants show systematic Hα/[N II] and [S II] λ6717/λ6731 variations independent of their galactocentric distances. These studies suggested that young, small-diameter remnants such as Kepler's SNR, the Crab Nebula, and Cas A have systematically lower Hα/[N II] and λ6717/λ6731 values than large, old objects like the Cygnus Loop, IC 443, and the Monoceros Loop. Omitting the young, ejecta-dominated remnants and including more recent spectral data, one still finds an apparent correlation between an SNR's Hα/[N II] and electron density–sensitive λ6717/λ6731 ratios. This is shown in Figure 6, where observed Hα/[N II] and λ6717/λ6731 ratio averages listed in Table 4 are plotted. The relation has a correlation coefficient of −0.70. A decrease in a remnant's filament density with increasing diameter and age (Daltabuit, D'Odorico, and Sabbadin 1976; Cantó 1977) correlated with lower shock velocities and hence less nitrogen release through grain destruction (Dopita 1977) was proposed as the cause for the correlation. On the other hand, a progressive dilution of an initially high nitrogen abundance in supernova ejecta with swept-up interstellar material has also been suggested to explain the observed relation (Bohigas 1983).

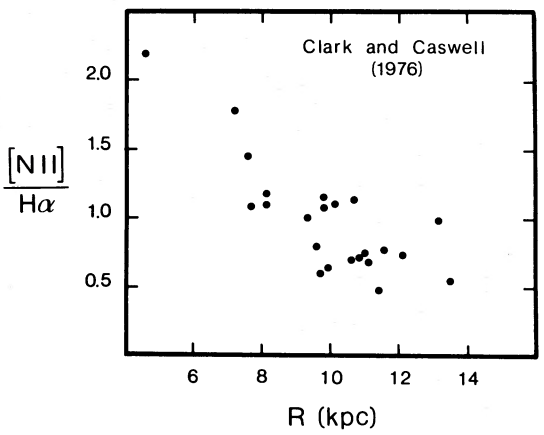

FIG. 5.—[N II]/Hα vs. galactocentric distance (*R*) for galactic remnants in our sample, using the distance estimates of Clark and Caswell (1976).

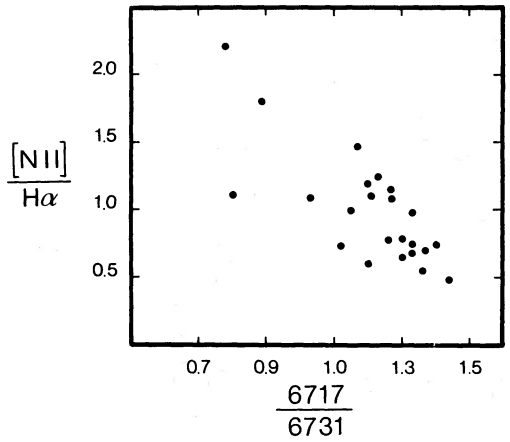

FIG. 6.—[N II]/Hα vs. the electron density–sensitive [S II] λ6717/λ6731 ratio for the galactic remnants in our sample (see Table 3).

The question to be answered then is, does [N II] emission intensity vary as a function of galactocentric distance owing to a general galactic nitrogen abundance gradient, or as a product of remnant evolution, or some combination of these two? We will show below that, although remnant evolution may affect its line-emission properties to some extent, the intensity of the [N II] lines appears to be dominated by swept-up interstellar medium abundance variations and that the [N II]/Hα correlation with remnant diameter and filament density is a result of observational selection effects.

Figures 7*a* and 7*b* show the [N II]/Hα and λ6717/λ6731 values from Table 4 plotted against remnant diameter using Clark and Caswell's (1976) estimates (with updates). Correlations of [N II]/Hα and λ6717/λ6731 with remnant size appear weak (Fig. 7*a*: correlation coefficient = −0.21; Fig. 7*b*: correlation coefficient = −0.31) and are certainly not as strong as earlier plots had indicated (e.g., Daltabuit, D'Odorico, and Sabbadin 1976). This results from the omission of young remnants from consideration as well as from the inclusion of more recent observational data. Therefore, although uncertainties of remnant diameters may affect the relation (cf. discussions on the Σ-*D* relation by Mills 1983 and Green 1984), the available data indicate little or no dependence of a remnant's filament density and [N II] emission strength upon diameter.

If evolutionary effects on [N II]/Hα strength and/or λ6717/λ6731 ratio were important for old remnants in general, one might also expect to observe an Hα/[N II] versus λ6717/λ6731 correlation in M31 and M33. Using data for M31 from Blair, Kirshner, and Chevalier (1981, 1982) and for M33 from Dopita, D'Odorico, and Benvenuti (1980) and Blair and Kirshner (1985), we show in Figure 8 the observed relation between [N II]/Hα and λ6717/λ6731 for these galaxies. No correlation appears to be present for M31 remnants (correlation coefficient = −0.21), while the M33 data indicate a possible trend (correlation coefficient = −0.62) but one that is considerably less steep than the galactic one. While the M31 remnants are quite similar to our galactic sample in terms of both diameter (>20 pc) and galactocentric distance, half of the M33 remnants have estimated diameters less than 10 pc. This makes

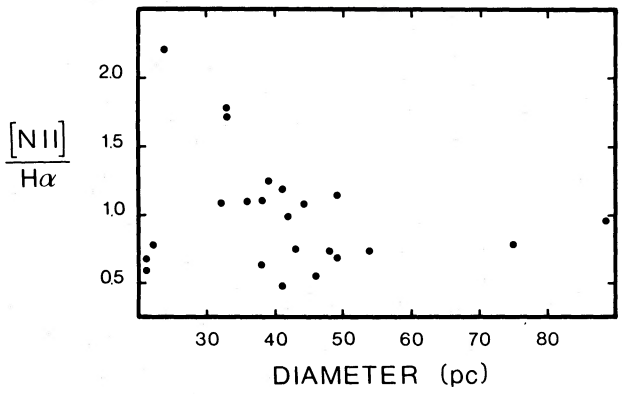

FIG. 7*a*

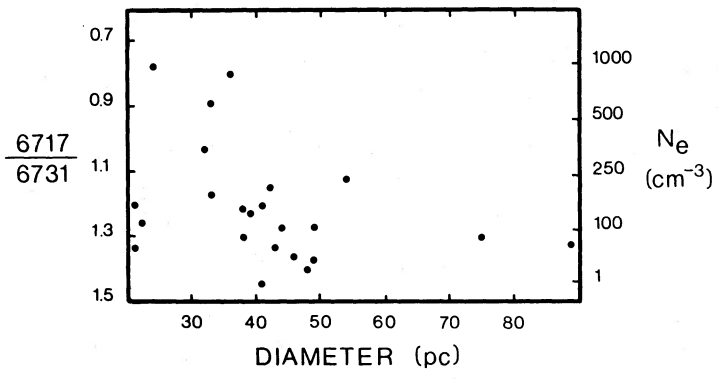

FIG. 7*b*

FIG. 7—(*a*) Observed [N II]/Hα and (*b*) the electron density–sensitive [S II] λ6717/λ6731 line ratio vs. remnant diameter for our sample of galactic remnants

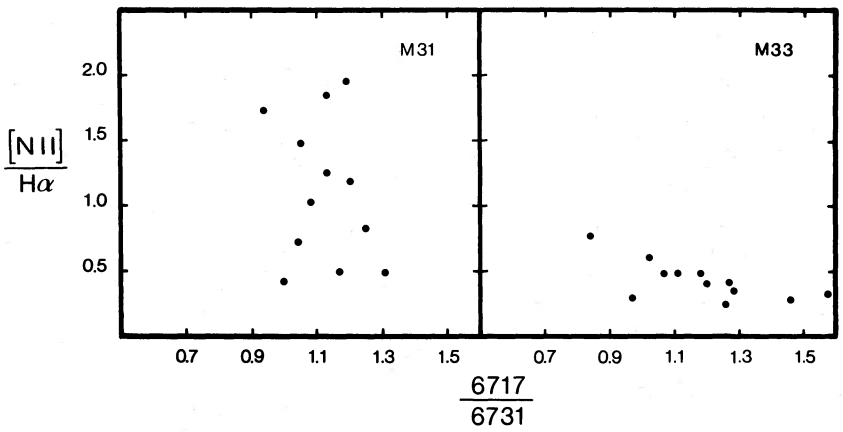

FIG. 8.—[N II]/Hα vs. λ6717/λ6731 for M31 and M33 remnants

it uncertain whether the M33 SNRs are representative of old remnants as in our galactic sample. Thus the meaning of any trend seen for M33 in Figure 8 similar to that seen for galactic remnants is ambiguous. Furthermore, Blair, Kirshner, and Chevalier (1982) investigated whether a relation exists between [N II]/Hα and remnant diameter for either galaxy, and concluded that if such a relation did exist, it is overwhelmed by each galaxy's nitrogen abundance gradient (see their Fig. 4). Therefore, evolutionary effects on the [N II]/Hα ratio are not supported by the M31 data and are only weakly supported by the M33 data.

Proposed evolutionary effects on the spectra of old remnants, such as grain destruction and ejecta dilution, do not appear, in fact, capable of accounting for more than a small percentage of the observed [N II] variations. For example, increased grain destruction in younger remnants due to higher shock velocities can not produce variations in the nitrogen emission of the size seen. Data for the ρ Oph line-of-sight direction suggests that nitrogen is depleted by about 50% in grains and molecules (Morton 1974, 1975), and recent theoretical studies by Seab and Shull (1983) suggest that a shock velocity of 120 km s^{-1} increases the postshock gas fraction of nitrogen from 50% to about 80%. While this may affect estimates of the absolute value of the galactic nitrogen abundance using SNRs as compared with H II regions (see abundance discussion below), the postshock nitrogen gas fraction difference due to shocks between 60 and 120 km s^{-1} (shock velocities typical of optical filaments) is a relatively small 13%, compared with the observed factor of 2 increase in the [N II]/Hα ratio.

Gradual dilution of a supernova's enriched ejecta with swept-up interstellar medium is proposed by Bohigas (1983) as the underlying cause for an observed decrease of nitrogen line strength from young to old remnants. Bohigas suggests that uniform mixing of ejecta with swept-up material occurs rapidly, resulting in an observed decrease in [N II]/Hα ratio with filament density, remnant diameter, and expansion velocity when one examines young and old remnants together. Thus, a gradual dilution of nitrogen-rich filaments from young, high-density filament remnants to old, low-density filament remnants would be observed, in addition to a galactic nitrogen abundance gradient. However, evolved SNR filaments are probably the result of a remnant's shock wave encountering an inhomogeneous interstellar medium. Highly efficient mixing of the presumed nitrogen ejecta with freshly shocked interstellar clouds would seem to be required in order to see evidence of nitrogen overabundance in the postshock recombination regions. Also, this mixing would lead to substantially shorter cooling times and lower postshock temperatures than were observed, whereas longer cooling times than predicted by steady-flow models appear to be suggested by the data (Fesen, Blair, and Kirshner 1982). Furthermore, theoretical models indicate that a reverse shock driven into the ejecta prevents the enriched material from keeping up with the blast wave (Gull 1973; McKee 1974; Chevalier 1975). Bohigas (1983) argues that despite such problems the remnants Puppis A and W50 indicate that ejecta are in fact not left behind. However, Puppis A is now known to be a relatively young remnant (Kirshner and Winkler 1985) possibly related to Cas A. Its nitrogen-rich knots are not ejecta (these are oxygen-rich and fast moving) but may instead be presupernova stellar wind material. In the case of W50, one has collimated beams of very high velocity material being ejected from the central object, which can catch and eventually pass the ever slowing blast wave shell.

The real cause for an apparent [N II]/Hα–λ6717/λ6731 trend may be simply observational selection effects. This has already been suggested by Binette *et al.* (1982), but they listed decreased reddening toward the anticenter direction and a galactic interstellar medium density gradient as the causes. The situation appears simpler than this. Figure 9 illustrates the observed increase in filament density (i.e., a λ6717/λ6731 ratio decrease) with decreasing galactocentric distance. This, when combined with a general galactic nitrogen abundance gradient, could result in the observed Hα/[N II] and density relation seen in Figure 6. The lack of a density–galactocentric distance (R) correlation for the remnants observed in M31 (Fig. 9) suggests an observational selection bias for galactic remnants. The trend seen for the galactic SNRs cannot be the result of a more rapid remnant development at large galactocentric distances as Binette *et al.* suggest. Otherwise, this trend should be present in M31 as well. Moreover, remnant development is probably more strongly dependent upon the local environment (Kafatos *et al.* 1980) than on a general galactic density gradient. Also, although interstellar reddening certainly plays an important role in optical remnant detection, there is enhanced concentration of optically visible SNRs toward the galactic center (van den Bergh 1983). In fact, the most distant optical remnant, RCW 103, with a distance of 8.7 kpc (Clark and Caswell 1976), lies near the galactic-center direction ($l = 332.^{\circ}4$).

The relation between Hα/[N II] and [S II] noted by Dalta-

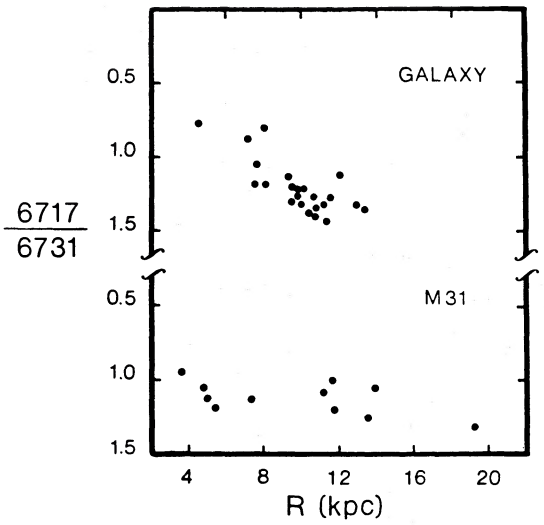

FIG. 9.—[S II] λ6717/λ6731 vs. galactocentric distance (R) for both galactic and M31 remnants.

buit, D'Odorico, and Sabbadin (1976) and others results from a selection bias of detecting smaller diameter, and higher density, filament remnants at small galactocentric distances, which consequently have higher nitrogen abundances owing to a galactic gradient. Since a remnant's optical emissivity (and hence its surface brightness) is proportional to filament density (cf. data of Kirshner and Arnold 1979), a derived electron density increase in [S II] toward the galactic center (see Fig. 9) is partially the result of the easier detection of the small, bright, and denser filament remnants in this direction. Small remnants near $l = 0°$ do in fact show higher filament densities. The average [S II] λ6717/λ6731 density for the inner six galactic remnants' filaments is 400 cm^{-3}, while it is only 100 cm^{-3} for the outer six. At the same time, there is a bias toward detecting smaller diameters remnants with decreasing galactocentric distance (R) as shown on the left-hand side of Figure 10, which makes use of the diameter data listed in Table 4. The average diameter for the six inner remnants is 33 pc, while it is 46 pc for the outer six. These same inner and outer groups of six remnants show a factor of 2 difference in [N II]/Hα ratio (1.50 inner and 0.75 outer). Because radio detection of SNRs is also limited by surface brightness, similar but less extreme bias for detecting smaller radio remnants with decreasing galactic distance is illustrated on the right-hand side of Figure 10, where we have plotted all galactic remnants using only the Clark and Caswell (1976) catalog data. Radio selection effects are discussed by Milne (1970), Downes (1971), Ilovaisky and Lequeux (1972), and Green (1984).

What is the slope of the galactic nitrogen abundance gradient from our sample of remnants, and how does it compare with those determined from H II regions? Binette *et al.* (1982) investigated galactic abundance gradients using evolved SNRs and found a nitrogen gradient of −0.095 dex kpc^{-1}, in good agreement with that determined using H II regions. However, as noted above, their sample included a few remnants of questionable reliability in determining an abundance gradient (i.e., W50, 3C 58, and OA 184). Furthermore, the abundances were derived from models of Dopita *et al.* (1984), which assume that [O III]/Hβ is sensitive to oxygen abundance and the hydrogen in the preshock medium is fully ionized (i.e., $V_s > 100$ km s^{-1}) as well as that steady flow conditions prevail for all remnants in the sample. Such assumptions are not likely to be valid in filaments exhibiting [O III]/Hβ ratios less than 1, indicative of relatively slow shocks (< 100 km s^{-1}), or greater than 10, suggesting nonsteady flows (Raymond *et al.* 1981; Fesen, Blair, and Kirshner 1982). Of their sample of 26 remnants, three exhibit small [O III]/Hβ ratios under 1.0 (W28, the Monoceros Loop, and Vela), five objects have no published [O III]/Hβ ratios at all (3C 400, W63, HB 3, HB 9, and G290.1−0.8), and two show predominantly very large [O III]/Hβ ratio filaments (G126.2+1.6 and CTA 1).

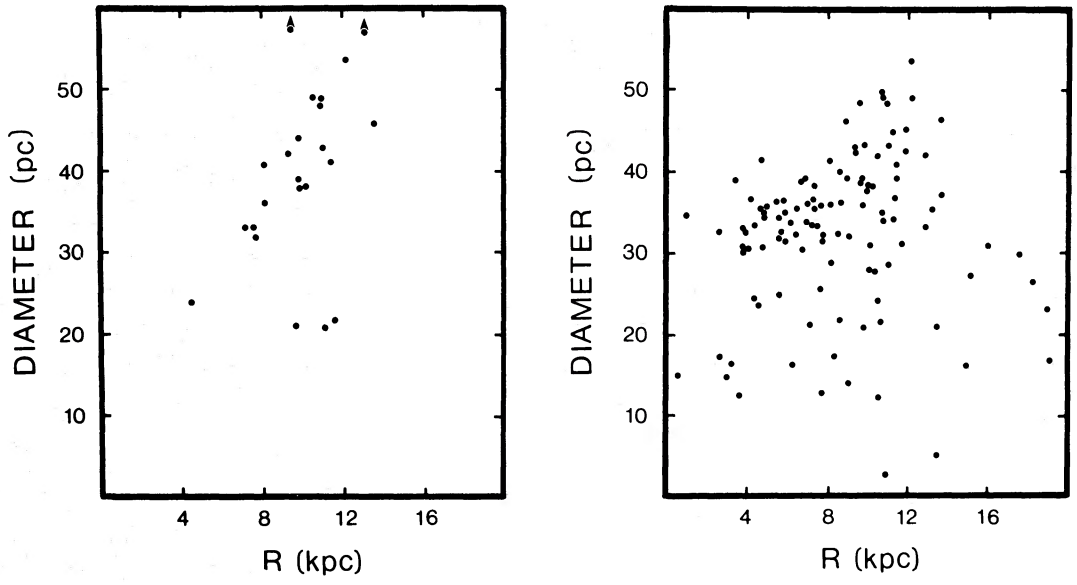

FIG. 10.—Remnant diameters as a function of galactocentric distance (R) for (*left*) the remnants in our sample and (*right*) all galactic remnants listed by Clark and Caswell (1976).

TABLE 6

ABUNDANCES IN GALACTIC SNRs

Remnant	R (kpc)	log [N II]/Hα	log λ6731/Hα	log [O III]/Hβ	Z(O) $\times 10^{-4}$	Z(N) $\times 10^{-5}$	Z(S) $\times 10^{-6}$	M	A
W28	7.7	0.04	−0.23	0.11	2.2	7.6	8.8	−0.08	−3.45
G65.3+5.7	9.6	−0.10	−0.32	0.34	3.7	6.4	8.6	−0.08	−3.45
Cygnus Loop	9.8	0.04	−0.40	0.67	9.0	12	15	0.31	−3.20
CTB 1	11.1	−0.17	−0.37	0.00	1.5	4.2	5.0	−0.54	−3.70
VRO 42.05.01	13.5	−0.25	−0.46	0.11	2.1	4.0	4.8	−0.60	−3.72
S147	10.9	−0.13	−0.31	0.25	2.8	5.4	7.7	−0.19	−3.50
IC 443	11.6	−0.11	−0.32	0.12	2.1	5.3	6.8	−0.30	−3.57
G206.9+2.3	12.1	−0.13	−0.37	0.68	9.0	8.5	18	0.18	−3.30
G296.1−0.7	9.8	0.10	−0.24	0.60	7.2	12	23	0.45	−3.18
RCW 86	8.1	0.05	−0.40	0.51	5.4	9.3	10	0.16	−3.32
RCW 89	7.2	0.25	−0.40	0.18	2.5	15	6.0	0.03	−3.30
RCW 103	4.6	0.35	−0.23	0.61	8.1	30	24	0.72	−2.60
MSH 15−56	7.6	0.17	−0.40	0.51	5.4	15	10	0.27	−3.50

If we omit these remnants from our sample, we are left with 13 remnants having spectral properties for their observed filaments at least consistent with Dopita *et al.*'s model assumptions. These remnants are listed in Table 6, along with their observed [N II], [S II] λ6731, and [O III] line ratios. Using the Dopita *et al.* (1984) abundance–line ratio diagrams, we have estimated nitrogen, oxygen, and sulfur abundances for these remaining remnants. The results are listed in Table 6 and plotted in Figures 11*a*, 11*b*, and 11*c*.

A least squares fit to the nitrogen abundances suggests $d \log (N/H)/dR = -0.088$ dex kpc^{-1}, with a correlation coefficient of −0.84. (Excluding RCW 103, which is the point in the upper left-hand corner, these values drop to −0.0755 dex kpc^{-1} and −0.73.) This nitrogen abundance gradient is similar to that derived by Binette *et al.* (1982) (even though they did not consider remnant [O III]/Hβ ratios in their analysis), as well as by others (see reviews in Binette *et al.*; Gonzales 1983, and Shaver *et al.* 1983). Thus it appears that, despite possible complicating factors, a galactic nitrogen abundance gradient like that observed with H II regions is obtained using SNRs. Blair and Kirshner (1985) have noted, however, that while the gradient derived from H II regions and SNRs may be similar, the absolute nitrogen abundances obtained from remnants are systematically higher by about a factor of 3–4. The nature of this discrepancy is presently unclear.

Although a reasonably well-defined trend in nitrogen abundance as a function of galactic distance appears to exist, there is no similar relation observed for oxygen or sulfur. This could be due to the small number of remnants left in the sample and/or the effects of slow shocks on the accuracy of derived

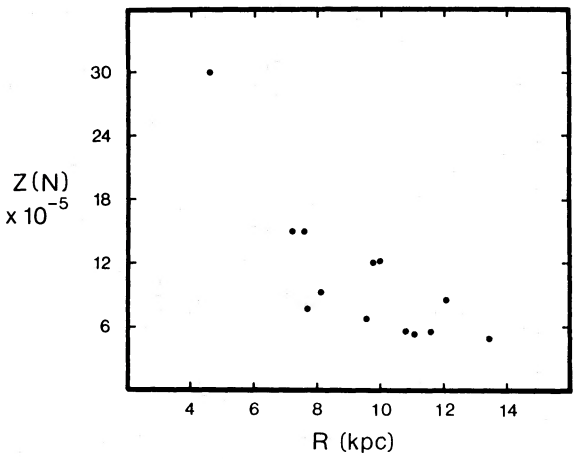

FIG. 11*a*

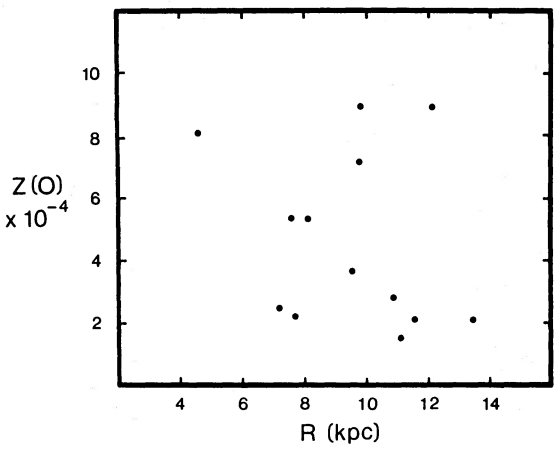

FIG. 11*b*

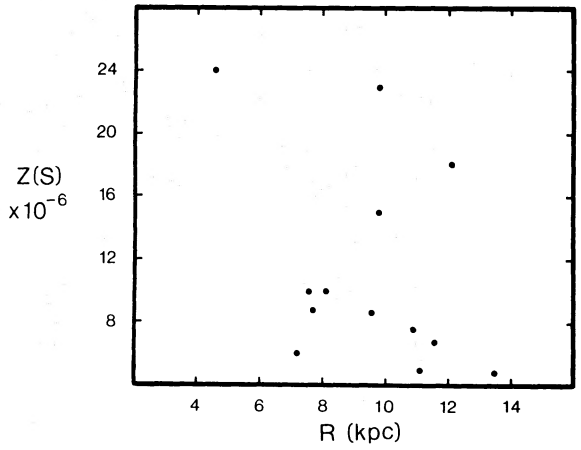

FIG. 11*c*

FIG. 11.—(*a*) Nitrogen, (*b*) oxygen, and (*c*) sulfur abundances for some of our sample remnants derived from Dopita *et al.*'s (1984) models

oxygen abundances using these models; six of the 13 remnants have [O III]/Hα ratios between 1 and 2. On the other hand, if the remnants' filaments represent nonsteady radiative shocks due to interstellar cloudlets, then these models may not yield reliable abundances.

Last, we calculated Dopita *et al.*'s (1984) metallicity (M) and metal abundance (A) parameters for each of the 13 remnants (see Table 6), and show in Figure 12 metal abundance as a function of galactic distance (R). The metal abundance parameter, which is the sum of the logarithmic abundances of N, O, and S, shows only a modest metal gradient toward the galactic center. Much of this observed gradient must be due to the nitrogen gradient, since there is little evidence for either an oxygen or a sulfur gradient (Figs. 11*b*, 11*c*; Binette *et al.* 1982, Fig. 2).

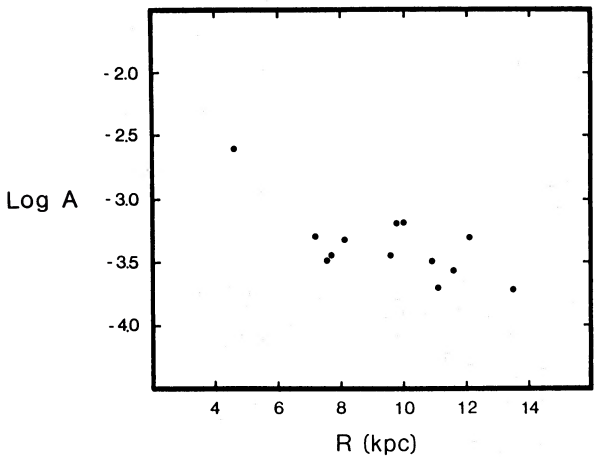

FIG. 12.—Total logarithmic remnant nitrogen, oxygen, and sulfur abundance (A) as a function of galactocentric distance (R).

V. CONCLUSIONS

We present spectrophotometric data for seven galactic remnants which substantially increase the quality and spectral coverage available on these objects. Distance estimates made by means of reddening measurements and general galactic extinction studies are largely consistent with estimates using the empirical radio Σ-D relation.

These new spectral data are combined with published data to investigate new line-ratio criteria for SNR identification. The [O I] and [O II] lines, when used together with the usual Hα/[S II] ratio test, seem to provide an excellent additional diagnostic tool for remnant discrimination from H II regions. This technique should be most useful for remnant identification in those cases where the Hα/[S II] ratio is ambiguous (i.e., $1.5 < \text{H}\alpha/[\text{S II}] < 2.5$).

We find also that, contrary to the suggestion of Daltabuit, D'Odorico, and Sabbadin (1976), the total range for observed Hα/[N II] and Hα/[S II] ratios within individual remnants is not negligible in relation to differences seen between remnants. However, mean values for each remnant appear well enough defined to permit remnant comparisons using a relatively small number of filament observations.

Good agreement exists between galactic nitrogen abundance gradients determined from H II regions and SNRs, despite the fact that those derived from remnants are subject to absolute abundance uncertainties. No galactic abundance gradients were found for oxygen and sulfur. Evolutionary-based variations in remnant nitrogen line strengths do not appear to be a significant factor compared with those caused by the galactic abundance gradient.

We thank Matt Johns for excellent assistance and support at McGraw-Hill Observatory, and J. C. Raymond and T. R. Gull for useful discussions. This research was funded in part by R. P. K.'s NSF grants AST 77-17600, AST 81-05050, and AST 83-09496.

REFERENCES

Angerhofer, P. E., Wilson, A. S., and Mould, J. R. 1980, *Ap. J.*, **236**, 143.
Baldwin, J. A., Phillips, M. M., and Terlevich, R. 1981, *Pub. A.S.P.*, **93**, 5.
Barker, T. 1978, *Ap. J.*, **219**, 914.
Binette, L., Dopita, M. A., D'Odorico, S., and Benvenuti, P. 1982, *Astr. Ap.*, **115**, 315.
Blair, W. P., and Kirshner, R. P. 1985, *Ap. J.*, **289**, 582.
Blair, W. P., Kirshner, R. P., and Chevalier, R. A. 1981, *Ap. J.*, **247**, 879.
———. 1982, *Ap. J.*, **254**, 50.
Blair, W. P., Kirshner, R. P., Fesen, R. A., and Gull, T. R. 1984, *Ap. J.*, **282**, 161.
Blair, W. P., Kirshner, R. P., Gull, T. R., Sawyer, D. L., and Parker, R. A. R. 1980, *Ap. J.*, **242**, 592.
Boeshaar, G. O., Boeshaar, P. C., Czyzak, S. J., Aller, L. H., and Lasker, B. M. 1980, *Ap. Space Sci.*, **68**, 335.
Bohigas, J. 1983, *Rev. Mexicana Astr. Ap.*, **5**, 271.
Bohigas, J., Ruiz, M. T., Carrasco, L., Salas, L., and Herrera, M. A. 1983, *Rev. Mexicana Astr. Ap.*, **8**, 155.
Cantó, J. 1977, *Astr. Ap.*, **61**, 641.
Caswell, J. L., and Lerche, I. 1979, *M.N.R.A.S.*, **187**, 201.
Chevalier, R. A. 1975, *Ap. J.*, **200**, 698.
———. 1977, *Ann. Rev. Astr. Ap.*, **15**, 175.
Chevalier, R. A., and Kirshner, R. P. 1979, *Ap. J.*, **233**, 154.
Clark, D. H., and Caswell, J. L. 1976, *M.N.R.A.S.*, **174**, 267.
Clark, D. H., and Stephenson, F. R. 1977, *The Historical Supernovae* (Oxford: Pergamon).
Daltabuit, E., D'Odorico, S., and Sabbadin, F. 1976, *Astr. Ap.*, **52**, 93.
Danziger, I. J., and Dennefeld, M. 1976, *Pub. A.S.P.*, **88**, 44.
Davidson, K. 1979, *Ap. J.*, **228**, 179.
Davies, R. D., Elliott, K. H., Goudis, C., Meaburn, J., and Tebbutt, N. J. 1978, *Astr. Ap. Suppl.*, **31**, 271.
Dennefeld, M. 1980, *Pub. A.S.P.*, **92**, 603.
Dennefeld, M., and Kunth, D. 1981, *A.J.*, **86**, 989.
D'Odorico, S. 1974, in *Supernovae and Supernova Remnants*, ed. C. B. Cosmovici (Dordrecht: Reidel), p. 283.
———. 1978, *Mem. Soc. Astr. Italiana*, **49**, 485.
D'Odorico, S., Benvenuti, P., and Sabbadin, F. 1978, *Astr. Ap.*, **63**, 63.
D'Odorico, S., Dopita, M. A., and Benvenuti, P. 1980, *Astr. Ap. Suppl.*, **40**, 67.
D'Odorico, S., and Sabbadin, F. 1976, *Astr. Ap.*, **53**, 443.
———. 1977, *Astr. Ap. Suppl.*, **28**, 439.
Dopita, M. A. 1977, *Astr. Ap.*, **56**, 303.
———. 1978, *Ap. J. Suppl.*, **37**, 117.
Dopita, M. A., Binette, L., D'Odorico, S., and Benvenuti, P. 1984, *Ap. J.*, **276**, 653.
Dopita, M. A., D'Odorico, S., and Benvenuti, P. 1980, *Ap. J.*, **236**, 628.
Dopita, M. A., Ford, V. L., McGregor, P. J., Mathewson, D. S., and Wilson, I. R. 1981, *Ap. J.*, **250**, 103.
Dopita, M. A., Mathewson, D. S., and Ford, V. L. 1977, *Ap. J.*, **214**, 179.
Downes, D., 1971, *A.J.*, **76**, 305.
Elliott, K. H., and Malin, D. F. 1979, *M.N.R.A.S.*, **186**, 45P.
Esipov, V. F., Kaplan, S. A., Lozinskaya, T. A., and Podstrigach, T. S. 1972, *Soviet Astr.—AJ*, **16**, 81.
Fesen, R. A. 1981, Ph.D. thesis, University of Michigan.
———. 1984, *Ap. J.*, **281**, 658.
Fesen, R. A., Blair, W. P., and Gull, T. R. 1981, *Ap. J.*, **245**, 131.
Fesen, R. A., Blair, W. P., and Kirshner, R. P. 1982, *Ap. J.*, **262**, 171.
Fesen, R. A., Blair, W. P., Kirshner, R. P., Gull, T. R., and Parker, R. A. R. 1981, *Ap. J.*, **247**, 148.
Fesen, R. A., Gull, T. R., and Ketelsen, D. A. 1983, *Ap. J. Suppl.*, **51**, 337.
Fesen, R. A., and Kirshner, R. P. 1980, *Ap. J.*, **242**, 1040.
FitzGerald, M. P. 1968, *A.J.*, **73**, 983.
Gonzales, J. 1983, *Rev. Mexicana Astr. Ap.*, **5**, 289.
Green, D. A. 1984, *M.N.R.A.S.*, **209**, 449.
Gull, S. F. 1973, *M.N.R.A.S.*, **162**, 135.

Gull, T. R., Kirshner, R. P., and Parker, R. A. R. 1977, *Ap. J. (Letters)*, **215**, L69.
Hawley, S. A. 1978, *Ap. J.*, **224**, 417.
Hawley, S. A., and Miller, J. S. 1977, *Ap. J.*, **212**, 94.
Henry, R., and MacAlpine, G. M. 1982, *Ap. J.*, **258**, 11.
Hester, J. J., Parker, R. A. R., and Dufour, R. J. 1983, *Ap. J.*, **273**, 219.
Ilovaisky, S. A., and Lequeux, J. 1972, *Astr. Ap.*, **18**, 169.
Kafatos, M., Sofia, S., Bruhweiler, F., and Gull, T. 1980, *Ap. J.*, **242**, 294.
Kaler, J. B. 1976, *Ap. J. Suppl.*, **31**, 517.
Kirshner, R. P., and Arnold, C. N. 1979, *Ap. J.*, **229**, 147.
Kirshner, R. P., and Chevalier, R. A. 1977, *Ap. J.*, **218**, 142.
Kirshner, R. P., Gull, T. R., and Parker, R. A. R. 1978, *Astr. Ap. Suppl.*, **31**, 261.
Kirshner, R. P., and Winkler, P. F. 1985, in preparation.
Kwitter, K. B., and Aller, L. H. 1981, *M.N.R.A.S.*, **195**, 939.
Kwitter, K. B., Jacoby, G. H., and Lawrie, D. G. 1983, *Pub. A.S.P.*, **95**, 732.
Landecker, T. L., Pineault, S., Routledge, D., and Vaneldik, J. F. 1982, *Ap. J. (Letters)*, **261**, L41.
Landecker, T. L., Roger, R. S., and Dewdney, P. E. 1982, *A.J.*, **87**, 1379.
Leibowitz, E. M., and Danziger, I. J. 1983, *M.N.R.A.S.*, **204**, 273.
Longmore, A. J., Clark, D. H., and Murdin, P. 1977, *M.N.R.A.S.*, **181**, 541.
Lozinskaya, T. A. 1972, *Soviet Astr.—AJ*, **15**, 910.
Lucke, P. B. 1978, *Astr. Ap.*, **64**, 367.
Mathewson, D. S., and Clarke, J. N. 1972, *Ap. J. (Letters)*, **178**, L105.
———. 1973, *Ap. J.*, **180**, 725.
McKee, C. F. 1974, *Ap. J.*, **188**, 335.
Mendoza, C., and Zeippen, C. J. 1982, *M.N.R.A.S.*, **198**, 127.
Miller, J. S. 1974, *Ap. J.*, **189**, 239.
Miller, J. S., and Mathews, W. G. 1972, *Ap. J.*, **172**, 593.
Mills, B. Y. 1983, in *IAU Symposium 101, Supernova Remnants and Their X-Ray Emission*, ed. J. Danziger and P. Gorenstein (Dordrecht: Reidel), p. 551.
Milne, D. K. 1970, *Australian J. Phys.*, **23**, 425.
———. 1979, *Australian J. Phys.*, **32**, 83.
Morton, D. C. 1974, *Ap. J. (Letters)*, **193**, L35.
———. 1975, *Ap. J.*, **197**, 85.
Neckel, T., and Klare, G. 1980, *Astr. Ap. Suppl.*, **42**, 251.
Oke, J. B. 1974, *Ap. J. Suppl.*, **27**, 21.
Osterbrock, D. E. 1958, *Pub. A.S.P.*, **70**, 180.
Osterbrock, D. E., and Costero, R. 1973, *Ap. J. (Letters)*, **184**, L71.
Parker, R. A. R. 1964, *Ap. J.*, **139**, 493.
———. 1967, *Ap. J.*, **149**, 363.
Parker, R. A. R., Gull, T. R., and Kirshner, R. P. 1979, *An Emission-Line Survey of the Milky Way* (NASA SP-434).
Peimbert, M. 1979, in *IAU Symposium 84, The Large-Scale Characteristics of the Galaxy*, ed. W. B. Burton (Dordrecht: Reidel), p. 307.
Peimbert, M., and Torres-Peimbert, S. 1977, *M.N.R.A.S.*, **179**, 217.
Peimbert, M., Torres-Peimbert, S., and Rayo, J. F. 1978, *Ap. J.*, **220**, 516.
Péquignot, D., and Dennefeld, M. 1983, *Astr. Ap.*, **120**, 249.
Pradhan, A. K. 1978, *M.N.R.A.S.*, **183**, 89P.
Raymond, J. C. 1979, *Ap. J. Suppl.*, **39**, 1.
———. 1983, *Adv. Space Res.*, **2**, 145.
Raymond, J. C., Black, J. H., Dupree, A. K., Hartmann, L., and Wolff, R. S. 1981, *Ap. J.*, **246**, 100.
Reich, W., Berkhuijsen, E. M., and Sofue, Y. 1979, *Astr. Ap.*, **72**, 270.
Reich, W., Kallas, E., and Steube, R. 1979, *Astr. Ap.*, **78**, L13.
Rosado, M. 1981, *Ap. J.*, **250**, 222.
———. 1982, *Rev. Mexicana Astr. Ap.*, **5**, 127.
Ruiz, M. T. 1981, *Ap. J.*, **243**, 814.
Sabbadin, F. 1976, *Astr. Ap.*, **51**, 159.
———. 1977, *Astr. Ap.*, **54**, 915.
Sabbadin, F., and D'Odorico, S. 1976, *Astr. Ap.*, **49**, 119.
Seab, C. G., and Shull, J. M. 1983, *Ap. J.*, **275**, 652.
Seward, F. D., Harnden, F. R., Murdin, P., and Clark, D. H. 1983, *Ap. J.*, **267**, 698.
Sharpless, S. 1959, *Ap. J. Suppl.*, **4**, 257.
Shaver, P. A., McGee, R. X., Newton, L. M., Danks, A. C., and Pottasch, S. R. 1983, *M.N.R.A.S.*, **204**, 53.
Sitnik, T. G., Klement'eva, A. Y., and Toropova, M. S. 1983, *Soviet Astr.*, **27**, 292.
Talent, D. L., and Dufour, R. J. 1979, *Ap. J.*, **233**, 888.
Tuohy, I. R., and Garmire, G. P. 1980, *Ap. J. (Letters)*, **239**, L107.
van den Bergh, S. 1960, *Zs. Ap.*, **51**, 15.
———. 1978, *Ap. J. Suppl.*, **38**, 119.
———. 1983, in *IAU Symposium 101, Supernova Remnants and Their X-ray Emission*, ed. J. Danziger and P. Gorenstein (Dordrecht: Reidel), p. 597.
Willis, A. G. 1973, *Astr. Ap.*, **26**, 237.
Woltjer, L. 1972, *Ann. Rev. Astr. Ap.*, **10**, 129.

WILLIAM P. BLAIR: Department of Physics, Rowland Hall, The Johns Hopkins University, Baltimore, MD 21218

ROBERT A. FESEN: Laboratory for Atmospheric and Space Physics, University of Colorado, Campus Box 392, Boulder, CO 80309

ROBERT P. KIRSHNER: Department of Astronomy, University of Michigan, Ann Arbor, MI 48109